# Development of High Temperature Superconducting Josephson Junction Device Technology

## Final Report

## January 1996 - January 1998

DuPont Superconductivity
NRL contract No. N00014-96-C-2005
Program Manager: Kirsten E. Myers

# REPORT DOCUMENTATION PAGE

*Form Approved*
*OMB No. 0704-0188*



| 1. AGENCY USE ONLY *(Leave blank )* | 2. REPORT DATE | 3. REPORT TYPE AND DATES COVERED |
|---|---|---|
| | 9 July 1998 | Final Report ; Jan '96 - Jan '98 |

4. TITLE AND SUBTITLE
Development of High Temperature Superconducting Josephson Junction Device Technology: Final Report - Draft

5. FUNDING NUMBERS

6. AUTHOR(S)
Dr. Kirsten E. Myers

7. PERFORMING ORGANIZATION NAME(S) AND ADDRESS(ES)
DuPont Superconductivity
Cenetral Research and Development
Route 141, Experimental Station
PO Box 80304
Wilmington, DE 19880-0304

8. PERFORMING ORGANIZATION REPORT NUMBER
Final Report

9. SPONSORING / MONITORING AGENCY NAME(S) AND ADDRESS(ES)
Naval Research Laboratory
Washington, DC 20375-5326

10. SPONSORING / MONITORING AGENCY REPORT NUMBER
CLIN 0002; DIN A006

11. SUPPLEMENTARY NOTES

12a. DISTRIBUTION / AVAILABLILITY STATEMENT
Unlimited Distribution

12b. DISTRIBUTION CODE
Code 3220, 6303, 6302, Dist List, DTIC, DCASMA, 5227

13. ABSTRACT *(Maximum 200 words)*

*The DuPont program was successful in generating useful knowledge about thallium cuprate materials, photoresist reflow processing, and radiant heater technology though it did not lead to a new junction technology. Among the achievements of this program was the in situ fabrication of both (Tl,Pb)Sr2CuO5 and (Tl,Pb)Sr2Ca1-xYxCu2O7 films on full two inch wafers. These films were uniform in properties and had quite smooth surfaces as predicted. We were also able to qualify cerium oxide as compatible with the in situ growth process and suitable in a thallium-based multilayer technology. In addition, this project resulted in the first-ever epitaxial thallium cuprate films with copper oxide sheets oriented out of the plane of the film. The program has determined that standard HTS substrates, NdGaO3, CeO2- buffered Al2O3, and LaAlO3, are not ideal for an in situ thallium cuprate junction technology. Moreover, we have found that (Tl,Pb)Sr2Ca1-xYxCu2O7 can be as susceptible to electromigration as YBa2Cu3O7. The potentially greater stability of (Tl,Pb)Sr2Ca1-xYxCu2O7 was considered to be one of the key benefits of developing this new technology. In conclusion, the development of stable, reproducible multilayer SNS junctions is no more likely to be achieved with the thallium lead cuprates than with any other HTS materials system.*

| 14. SUBJECT TERMS | 15. NUMBER OF PAGES |
|---|---|
| Thallium Lead Cuprates; Superconductors; Thin films: TlPb-1201, TlPb-1212 | 60 |
| | 16. PRICE CODE |

| 17. SECURITY CLASSIFICATION OF REPORT | 18. SECURITY CLASSIFICATION OF THIS PAGE | 19. SECURITY CLASSIFICATION OF ABSTRACT | 20. LIMITATION OF ABSTRACT |
|---|---|---|---|
| | | | |

DuPont Superconductivity
Experimental Station E304/C121
Wilmington, DE 19880-0304
Tel. (302) 695-3704
Fax (302) 695-2721

DuPont Superconductivity

July 9, 1998

Defense Technical Information Center
8725 John J. Kingman Rd. #944
Fort Belvoir, VA 22060-6217

Subject: Final Report for Contract No. N00014-96-C-2005

To Whom It May Concern:

Enclosed are the SF 298 (Report Documentation Page) and 4 copies of the Final Report for the subject contract.

Yours truly,

J. William Cowdright
Administrative Manager
DuPont Superconductivity

# Material Inspection and Receiving Report

| 1. PROC. INSTRUMENT IDEN. (CONTRACT) | (ORDER) NO. | 6. INVOICE | 7. PAGE | OF |
|---|---|---|---|---|
| N00014-96-C-2005 | 63-6381-95 | | 1 | 1 |
| | | | 8. ACCEPTANCE POINT: D | |

| 2. SHIPMENT NO. | 3. DATE SHIPPED | 4. B/L | 5. DISCOUNT TERMS |
|---|---|---|---|
| KEM002Z | 9 Jul 1998 | TCN | N/A |

| 9. PRIME CONTRACTOR | CODE | 10. ADMINISTERED BY | CODE |
|---|---|---|---|
| DuPont Superconductivity<br>Central Research & Development<br>Route 141, Experimental Station<br>Wilmington, DE 19880-0304 | 8B460 | DCMC - PHiladelphia<br>PO Box 7699<br>Philadelphia, PA 19145-7699 | S3915A |

| 11. SHIPPED FROM (If other than 9) | CODE | FOB: | 12. PAYMENT WILL BE MADE BY | CODE |
|---|---|---|---|---|
| | | | DFAS Columbus Center<br>DFAS-CO-JNF/New Dominion Division<br>PO Box 182041<br>Columbus, OH 43218-2041 | SC1014 |

| 13. SHIPPED TO | CODE | 14. MARKED FOR | CODE |
|---|---|---|---|
| Defense Technical Information Center<br>8725 John J. Kingman Rd #944<br>Fort Belvoir, VA 22060-6217 | | | |

| 15 ITEM NO. | | 16. STOCK/PART NO. DESCRIPTION (Indicate number of shipping containers - type of container - container number) | 17 QUANTITY SHIP/REC'D* | 18 UNIT | 19 UNIT PRICE | 20 AMOUNT |
|---|---|---|---|---|---|---|
| CLIN | 002 | | | | $ | $ |
| DIN | A006 | Final Report | 4 | Rpt | | |

| 21 PROCUREMENT QUALITY ASSURANCE | | | 22 RECEIVER'S USE |
|---|---|---|---|
| A. ORIGIN<br>☐ PQA ☐ ACCEPTANCE of listed items has been made by me or under my supervision and they conform to contract, except as noted herein or on supporting documents. | B. DESTINATION<br>☐ PQA ☐ ACCEPTANCE of listed items has been made by me or under my supervision and they conform to contract, except as noted herein or on supporting documents. | | QUANTITIES SHOWN IN COLUMN 17 WERE RECEIVED IN APPARENT GOOD CONDITION EXCEPT AS NOTED. |
| DATE RECEIVED / SIGNATURE OF AUTHORIZED GOVT REP | DATE RECEIVED / SIGNATURE OF AUTHORIZED GOVT REP | | DATE RECEIVED / SIGNATURE OF AUTHORIZED GOVT REP |
| TYPED NAME AND OFFICE | TYPED NAME AND OFFICE | | TYPED NAME AND OFFICE |
| | | | *If quantity received by the Government is the same as quantity shipped, indicate by (√) mark, if different, enter actual quantity received below quantity shipped and encircle.* |

23. CONTRACTOR USE ONLY

# TABLE OF CONTENTS

## 1. Executive Summary

The Development of High Temperature Superconducting Josephson Junction Device Technology program was successful in generating useful knowledge about thallium cuprate materials, photoresist reflow processing, and radiant heater technology though it did not lead to a new junction technology. Among the achievements of this program was the *in situ* fabrication of both $(Tl,Pb)Sr_2CuO_5$ and $(Tl,Pb)Sr_2Ca_{1-x}Y_xCu_2O_7$ films on full two inch wafers. These films were uniform in properties and had quite smooth surfaces as predicted. We were also able to qualify cerium oxide as compatible with the *in situ* growth process and suitable in a thallium-based multilayer technology. In addition, this project resulted in the first-ever epitaxial thallium cuprate films with copper oxide sheets oriented out of the plane of the film.

The DuPont program has determined that the standard HTS substrates, neodymium gallate, cerium oxide-buffered sapphire, and lanthanum aluminate, are not ideal for an *in situ* thallium cuprate junction technology. Moreover, we have found that $(Tl,Pb)Sr_2Ca_{1-x}Y_xCu_2O_7$ can be as susceptible to electromigration as $YBa_2Cu_3O_7$. The potentially greater stability of TlPb-1212 was considered to be one of the key benefits of developing this new technology. In conclusion, the development of stable, reproducible multilayer SNS junctions is no more likely to be achieved with the thallium lead cuprates than with any other HTS materials system.

## 2. Technical Results

The goal of the program was to develop novel thallium cuprate Ramp SNS junctions using superconducting (Tl,Pb)$Sr_2Ca_{1-x}Y_xCu_2O_7$ (TlPb-1212), $CeO_2$ as the insulator, and (Tl,Pb)$Sr_2CuO_5$ (TlPb-1201) as the normal metal. While the program was successful in generating some unique materials and useful information on a variety of topics relevant to general HTS technology, it did not lead to the envisioned thallium cuprate junction technology.

Highlights of the technical successes include the *in situ* fabrication of both TlPb-1201 and TlPb-1212 films on full two inch wafers, the demonstration of cerium oxide on TlPb-1212 and TlPb-1212 on cerium oxide bilayers, and the epitaxial growth of 110 oriented thallium cuprate films on sapphire ($Al_2O_3$). Among the key learnings of this work are the geometry-dependent nature of the resist reflow process, the disappointing mechanical properties of neodymium gallate ($NdGaO_3$), and the ease of potassium substitution in, and electromigration of, TlPb-1212.

The data collected during the two years of the program can be grouped into the following six areas: Processing, which includes photoresist reflow processing and ion milling studies, Radiant Heater Technology, Substrates, the *In situ* Growth Process, *In situ* Growth Results, and Thallium Cuprate

Materials generally. The program's main results are presented and discussed in the sections below according to these categories.

## 2.1. Processing

The typical procedure for making SNS Ramp junctions requires the formation of a shallow sidewall or ramp in a superconductor / insulator bilayer. A standard procedure involves a "reflow" step in which a patterned photoresist layer is heated to the point that the resist flows a small, controlled amount. As the resist flows, the sidewalls of the film become rounded and shallower. The pattern is then transferred into the bilayer via ion-milling, though wet etching can also be used. These two steps involve several laboratory and materials-specific parameters. Measurement of these parameters allowed us to establish a ramp processing procedure, though it was never proven out in full junction fabrication.

### *2.1.1. Photoresist Reflow Processing*

Atomic Force Microscopy (AFM) was used to measure the sidewall angles of patterned resist samples. A two inch diameter silicon wafer was spin-coated with AZ S1813 and patterned under standard conditions. For S1813 resist and normal exposure and development times, the sidewall angle was about 40° ± 3° (measured from the plane of the substrate). The wafer was then cleaved and the pieces subjected to reflow under different conditions.

After reflow, the profile of the resist is curved making the definition of a sidewall angle problematic. Given the similar ion-milling rates of TlPb-1212, $CeO_2$, and resist (see Section 2.1.2 below), the shape of only the lower ≈ 300 nm of resist is important. This part of the profile tends to be straight. We therefore defined the sidewall angle as the Arctan of 300 nm divided by the lateral distance in nm from the bottom of the sidewall to the point where the resist was 300 nm thick.

In a first series, the resist was reflowed in an oven at 135 °C for times of 5 to 30 minutes. We found that the sidewall angle is not strongly influenced by the time duration of the reflow. The reflow time in subsequent studies was therefore shortened to 5 minutes. Next, the temperature of the oven was varied from 125 to 155 °C. Figure 2.1.1.a plots the sidewall angle as a function of reflow temperature (T = 0 corresponds to samples that were not reflowed). As expected, the sidewall angle shallows with increased reflow temperature. The range of angles formed, from 42 to 22°, encompasses the range of angles that we intend to study.

A third series of samples were then subjected to reflow at 140, 150 and 155 °C. The only difference between these samples and those in the second series was that the patterned photoresist had been allowed to age for 7.5 weeks. Figure 2.1.1.b shows that a reflow of the aged photoresist tended to produced shallower sidewalls. This indicates the importance of process consistency.

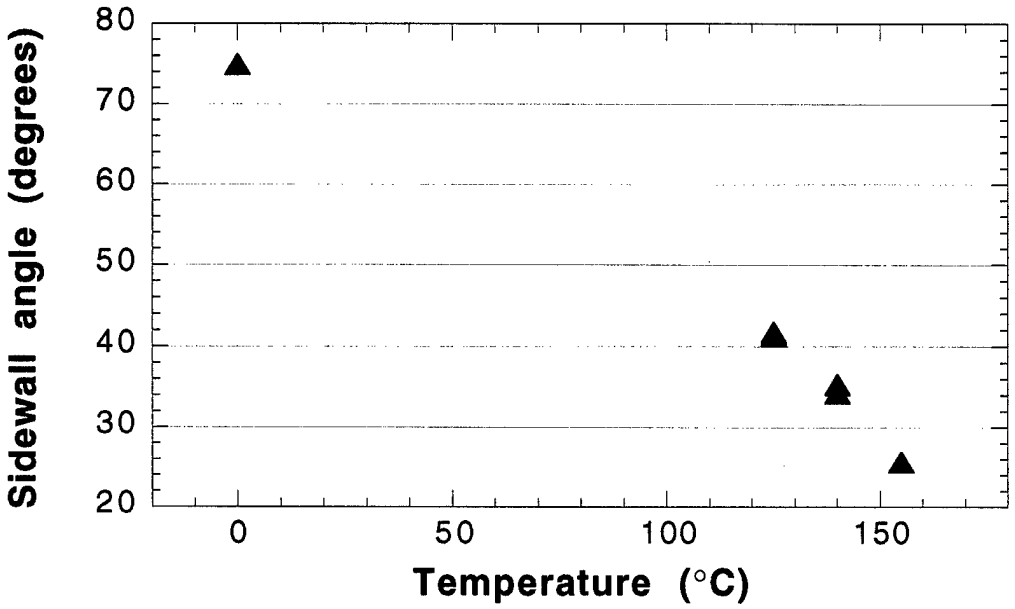


Figure 2.1.1.a: The effect of reflow temperature on the sidewall angle of S1813 photoresist.

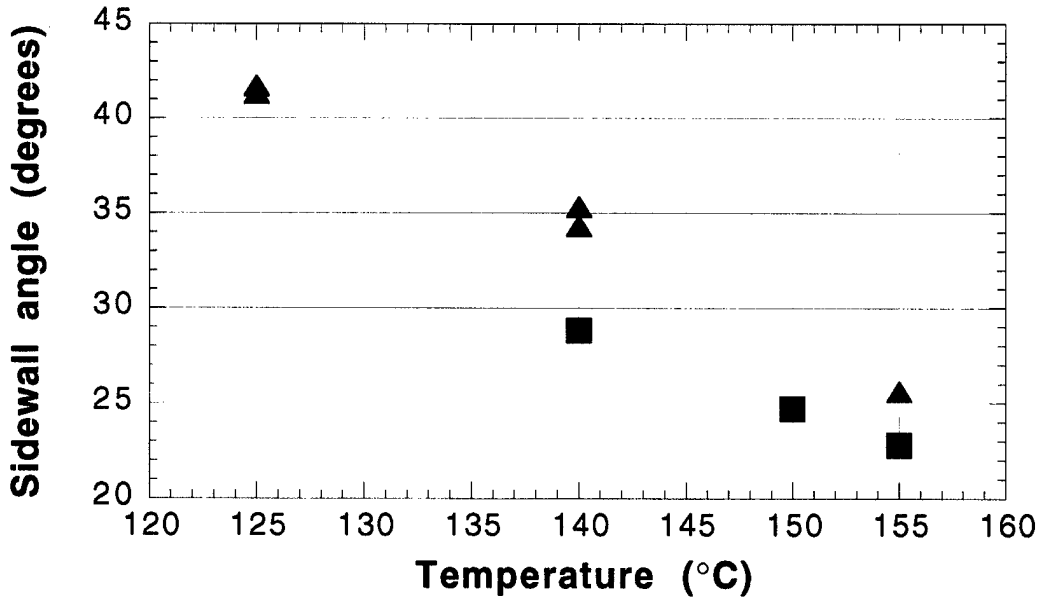


Figure 2.1.1.b: The effect of photoresist aging on reflow profile. Triangles: reflowed immediately after patterning; squares: reflowed 7.5 weeks after patterning.

All of the sidewall angles plotted in Figures 2.1.1.a and b were measured on the sides of features that were 20 microns wide. We found, as have others, that the shape of the reflowed lines are a function of the feature size (Figure 2.1.1.c). Wider line broaden symmetrically and there is a slight hump at the top of either side of the resultant trapezoid. Lines narrower than about 20 microns become asymmetric, developing a very broad (4 - 8 μm), shallow feature on one or both sides. We also note that the effective angle at a corner is shallower than along a straight edge.

The dependence of the sidewall angle on feature geometry has several important implications. First of all, one must be careful in trying to interpret junction data, particularly the scaling of junction parameters with junction area, if this process is used. Secondly, one must be careful in circuit layout as any edge patterned during this step will have feature-size dependent edges which could impact line critical current or inductance, for example.

### 2.1.2. *Ion Milling Rates*

We intended to transfer the reflowed resist pattern to the TlPb-1212 / $CeO_2$ bilayer via $Ar^+$ ion-milling. It is important to know the etch rates of all of the materials involved. Widely disparate etch rates could result in poor transfer of the critical sidewall angle.

The etch rates of TlPb-1212, $CeO_2$, and S1813 photoresist were measured as a function of ion beam angle. The angle of the incident beam relative to the substrate normal was varied from 0 to 60°. The beam energy and current were kept as low as possible, 200 eV and 200 mA, to minimize damage to the patterned ramp. The results are shown in Table 2.1.2.a. An incidence angle of 45° was chosen as the etch rates of TlPb-1212 and $CeO_2$ are comparable (38 and 45 Å/min. respectively) and are only 22 to 44% lower than that of S1813. Etching at 45° with rotation should allow for uniform etching with a minimum of redeposition.

Table 2.1.2.a: Etch rates (in Å/min.) of different materials as a function of beam angle. Beam voltage and current were 200 eV and 200 mA, respectively.

| Material | 0° | 45° | 60° |
|---|---|---|---|
| TlPb-1212 | 63 | 38 | 34 |
| CeO2 | 44 | 45 | 22 |
| S1813 | | 55 | 39 |

## 2.2. Radiant Heater Technology

An integral part of this program was the installation of a radiant heater in the *in situ* deposition system. The benefits of the radiant heater were expected to be the ability to make larger area, more uniform films, higher yields, lower photolithography costs, and an increased operating temperature range.

Previously, the substrates were attached to a sample heater with silver paint. The use of silver paint limited the substrate size to half inch squares and resulted in a high yield loss due to breakage during removal. The old heater could not be rotated or moved relative to the targets.

We designed a radiant heater specifically for this program to meet the size constraints of the *in situ* chamber and allow deposition on two inch diameter substrates. The new heater was designed to rotate the sample during deposition, providing better compositional and thickness uniformity as well as better step coverage. We also provided a means of vertical translation relative to the targets to optimize growth conditions.

### *2.2.1. Deposition Uniformity*

Following installation of the new heater, one of the first items to be addressed was that of film uniformity, both in terms of thickness and composition. The deposition chamber is such that the gun to substrate angle is fixed at 90°. However, the sputtering guns may be moved in or out and the new substrate heater can be raised or lowered. The pressure during film growth also has a significant impact on the deposition pattern. Lower pressures gave more uniform deposition, but the cost was poorer film quality (all else being equal). In the end, we compromised at 150 mtorr. With proper adjustment of the translation of the stage, we were able to produce reasonable films with less

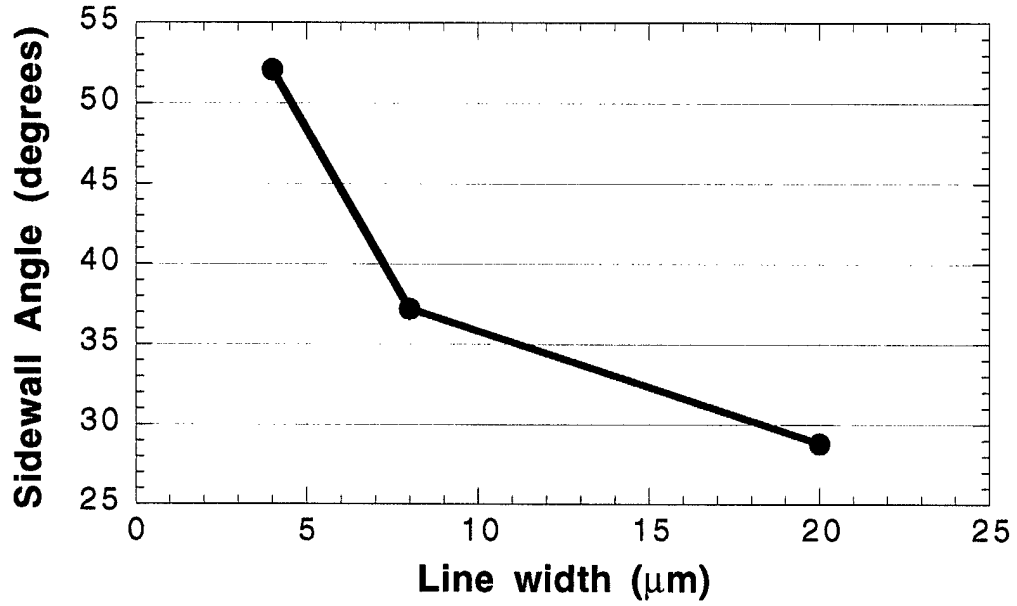


Figure 2.1.1.c: The effect of feature size on sidewall angle.

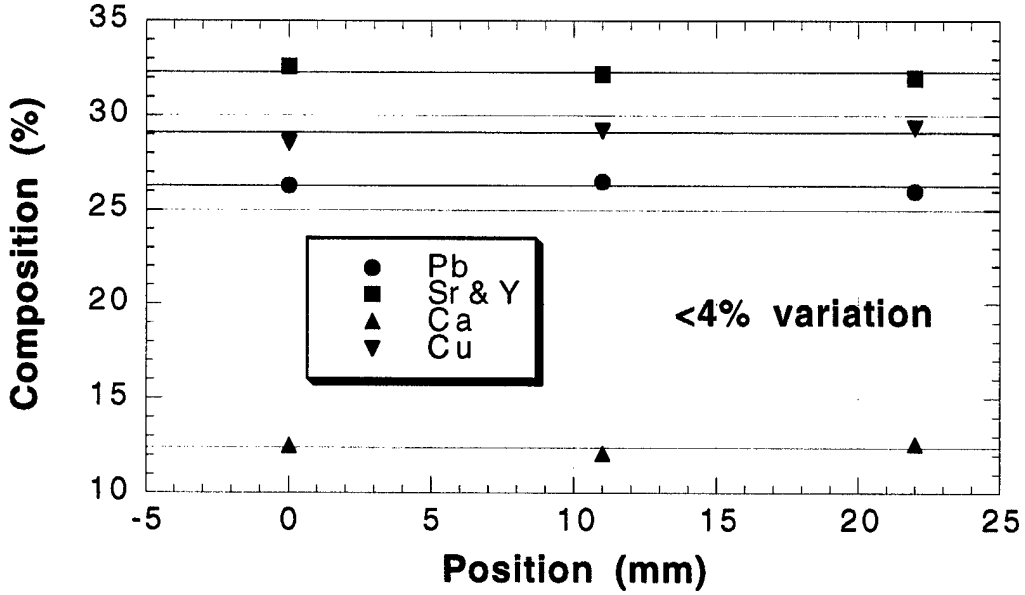


Figure 2.2.1.a: Compositional uniformity of TlPb-1212 deposition across a two inch wafer.

than an 8% variation in thickness and composition across the full 2" wafer (see Figure 2.2.1.a).

### 2.2.2. *Radiative Element*

At the start of the program, we faced the decision of which type of radiant heater to install. Our previous experience with quartz lamp heaters for YBCO deposition was quite good, and a new generation promised to be even better. However, we also knew that thallium reacts vigorously with quartz under the conditions likely to be extant in the growth chamber. One of our colleagues suggested that the heaters he had used, based on Kanthal Super elements, would be a better choice. His experience was that they lasted longer and required less maintenance than quartz lamp heaters, a definite benefit for our system.

Unfortunately, we have experienced a whole host of difficulties with the heater design based on a Kanthal Super SWR element. The back of the vendor-supplied heater element was not sufficiently well-insulated from the front and as a result the back of the heater became quite hot, raising the possibility that the electrical leads might melt. We modified the design to increase radiative heat loss, increased the insulation between the two sides of the heater, and replaced the vendor-supplied aluminum alloy leads with gold leads. In the end, even these changes were insufficient.

The elements themselves are extremely fragile, particularly after they have been used. Moreover, the Kanthal Super material sags with thermal cycling if not supported from below and the vendor-supplied elements were not supported at all, except from the electrical connections. We made several attempts to secure the elements, but meanwhile two elements failed causing delays to the program. The vendor was generally unresponsive to our concerns and replacement lead times were far too long.

In addition, we have to consider that the wafer cracking problem (discussed in detail in Section2.3 below) may be related in part to the radiation spectrum of the radiative element. The Kanthal Super element operates at a lower effective temperature than quartz lamps so that the radiation spectrum is shifted to longer wavelengths. We expected that this would result in increased efficiency of the heater as the substrates in question, $NdGaO_3$, $LaAlO_3$, and $Al_2O_3$, have higher absorption at longer wavelengths. However, it is possible that the increased absorption lead directly to increased thermal gradients, stress, and eventual fracture.

## 2.3. Substrates

Prior to the start of this program, our highest transition temperature ($T_c$) *in situ* films had been grown on $LaAlO_3$. Unfortunately, the location of twin boundaries in $LaAlO_3$ can move during high temperature deposition steps.

Across a two inch wafer, patterned features can shift by as much as 5 μm making alignment of multilayer structures impossible. Thus $LaAlO_3$ was deemed unacceptable for junction fabrication.

### 2.3.1. *Neodymium gallate*

Neodymium gallate was the substrate material originally chosen for this project. It was initially thought to be the best choice of substrate based on the substrate lattice match, chemical compatibility, and lack of twinning. Unfortunately, two inch $NdGaO_3$ wafers do not seem to be able to survive the required temperature and pressure conditions, at least not in our current deposition chamber. Other labs have reported similar difficulties which leads us to believe that the problem is with the material's intrinsic brittleness, weakness, or low thermal conductivity, though the heater itself may play a role as mentioned above.

We first had the problem that the wafer shattered during the oxygen backfill. This seemed to be due to mechanical or thermal stress put on the wafer by the large in-rush of cool gas. The problem was circumvented by a combination of cooling the wafer prior to backfilling and reducing the gas inlet rate.

We then found that the $NdGaO_3$ wafers would crack when the pressure was stable, but high (500 Torr) and the temperature was being raised. We reported in March, 1997 that the use of a sapphire wafer behind, and in direct contact

with, the $NdGaO_3$ wafer to be deposited on allowed these wafers in survive thermal cycling to 900°C in 500 Torr $O_2$ (the anneal conditions). Unfortunately, this approach has several difficulties. One is that if the two wafers stick together, which happens not infrequently, one or both break. Also the transparency of the sapphire window changes with thermal cycling so that the sapphire could not be reused. Even worse, as soon as a good quality film is grown on the $NdGaO_3$ wafer, the cracking problem returned. If the deposition conditions were off, so that the film was insulating, it would not crack. Paranoid as this may seem, it is true. The reason seems to be that the good, conducting film absorbs more radiant energy and therefore becomes hotter relative to the uncoated side. When the chamber is at low pressure (during deposition), this is not a problem. However, at high pressure (during anneal), convection becomes an important heat transfer mechanism and seems to be working to aggravate the thermal gradiant across the substrate.

Later we tried using a thick quartz plate just above, but *not* in direct contact with the substrate. This helped in that it raised the temperature at which a wafer would crack. We then tried an anneal with the thallium source completely removed from the chamber. We hypothesized that since the thallium source takes up a lot of the volume of the chamber, removing it would change the gas flow pattern, hence convective heat transfer, in the chamber dramatically. Indeed, we found that wafers could survive an anneal in this configuration. Obviously however, we need a thallium source for the growth, and possibly during the anneal (although it is not heated, and

therefore much cooler than the substrate, it may still contribute to a background thallous oxide partial pressure).

The next step was to return the thallium source to the chamber, but to cover it with a thin Inconel shutter during the anneal. This seemed to allow wafers to survive the anneal as well. We thus settled on a procedure of placing a quartz sheet above the wafer and an Inconel shutter below the wafer during the anneal.

In the course of the program, we tried many different things to try to eliminate the breakage. Occasionally $NdGaO_3$ wafers survived the process, but then the problem would reappear. In light of this situation, we felt it critical to explore other ways to circumvent the problem. One way was to switch to other substrate materials. Some films were grown on $LaAlO_3$ (see Section ??), but it too suffered breakage problems. We also explored the use of cerium oxide-buffered sapphire substrates which are stronger and have higher thermal conductivity.

### 2.3.2. *Cerium Oxide-Buffered Sapphire*

In order to grow HTS materials on sapphire, it is important to deposit a buffer layer first to eliminate interface reactions between the substrate and film. Cerium oxide is typically used as a buffer for this purpose.

The cerium oxide buffer layer was grown either in the *in situ* system or in a separate deposition system using a process developed for YBCO films. After deposition, the 100 orientation of the $CeO_2$ was verified. The width of the rocking curve of the $CeO_2$ 200 peak varied in these experiments, but did not have a dramatic impact on the final TlPb-1212 films.

A purely 110-oriented, epitaxial TlPb-1212 film was grown at a heater temperature of 680°C with a 60 nm YBCO absorbing film on the backside of the sapphire wafer. The thallous oxide condensation rate was 6.0 nm/s. After deposition, the chamber was backfilled to 500 T with $O_2$ and then the heater temperature was ramped up to 910°C for 60 min. The thallium source was not covered nor heated during the anneal.

Figure 2.3.2.a is a x-ray diffraction $\theta$-$2\theta$ scan for a 100 oriented $CeO_2$ film on a r-plane sapphire substrate. The inset shows an $\omega$-scan through the 200 peak of the $CeO_2$ film with a FWMH of 0.57°. The $\theta$-$2\theta$ scan for a 110 oriented TlPb-1212 film on $CeO_2$ on sapphire is shown in Figure 2.3.2.b. The peak at 33.15° includes intensity from both the 110 peak of TlPb-1212 and the 200 peak of $CeO_2$. The TlPb-1212 220 and $CeO_2$ 400 peaks also overlap at about 69.5°. The other two peaks, at 25.57° and 52.55°, are from the substrate. The rocking curve FWMH for the TlPb-1212 110 peak was 1.1° as shown in the inset. The 103 peaks of the TlPb-1212 film are found at $2\theta = 32.44°$ and $\chi = 59.0°$. A phi scan through the 103 peaks is shown in Figure 2.3.2.c along with a phi scan through the 111 peaks of the $CeO_2$ film.

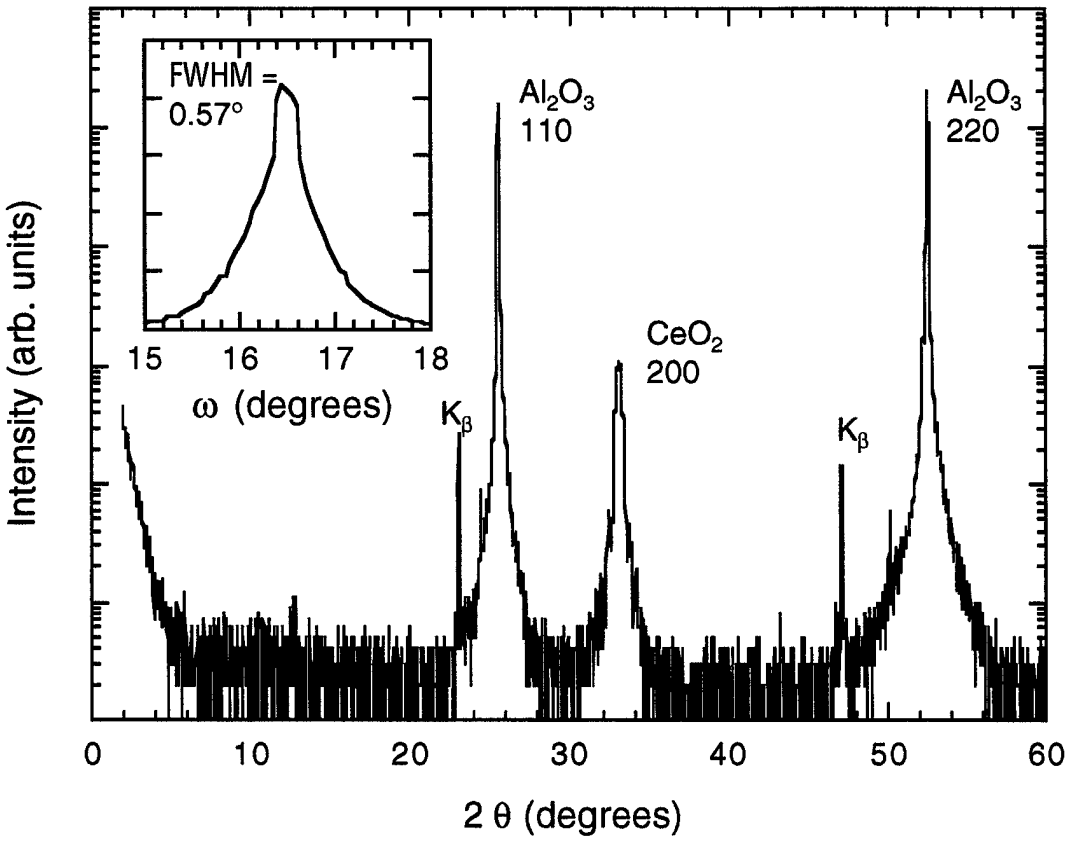


Figure 2.3.2.a: A θ-2θ scan of 100-oriented $CeO_2$ on r-plane $Al_2O_3$. The inset shows an ω-scan through the 200 peak of $CeO_2$.

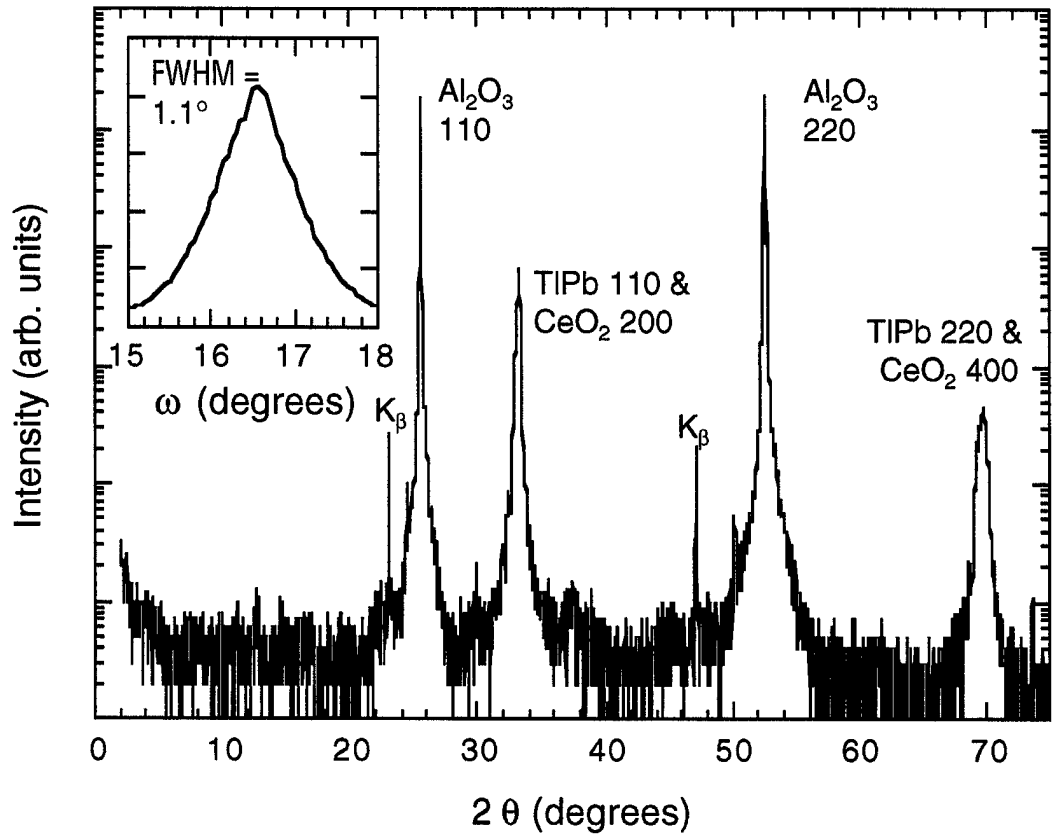


Figure 2.3.2.b: A θ-2θ scan of 110-oriented TlPb-1212 on 100-oriented $CeO_2$ on r-plane $Al_2O_3$. The inset shows an ω-scan through the overlapping 110 peak of TlPb-1212 and 200 peak of $CeO_2$.

Figure 2.3.2.c proves that the TlPb-1212 film is oriented cube-on-cube to the $CeO_2$ buffer layer, but with two different in-plane orientations: c-axis along 0° and c-axis along 90°. A schematic of the two crystallite orientations is shown in Figure 2.3.2.d. The different intensities of the two sets of TlPb-1212 103 reflections appears to be real suggesting some degree of preferential orientation of the c-axis of the TlPb-1212.

Figure 2.3.2.d: Schematic of growth of TlPb-1212 on $CeO_2$ on r-plane sapphire showing two preferred and distinct in-plane orientations.

Figure 2.3.2.e is an Atomic Force Micrograph of the surface of an 800 Å thick TlPb-1212 film. While there is some roughness to the surface, it is much less than for *ex situ* processed thallium cuprate films, on the order of 10% of the thickness of the film.

Unfortunately, the 110-oriented wafers were not superconducting. Moreover, the orientation of the copper oxide planes is not optimal for ramp type junctions. Naturally, we sought to determine conditions that would allow growth of pure 001-oriented TlPb-1212 on $CeO_2$-buffered sapphire. We varied the growth temperature, deposition rate, and anneal temperatures of the TlPb-1212. We also varied the growth conditions for the $CeO_2$ buffer layer. Under most conditions, we obtained mixed-orientation TlPb-1212 films and under no conditions were we able to get more than about 10 % c-axis oriented growth.

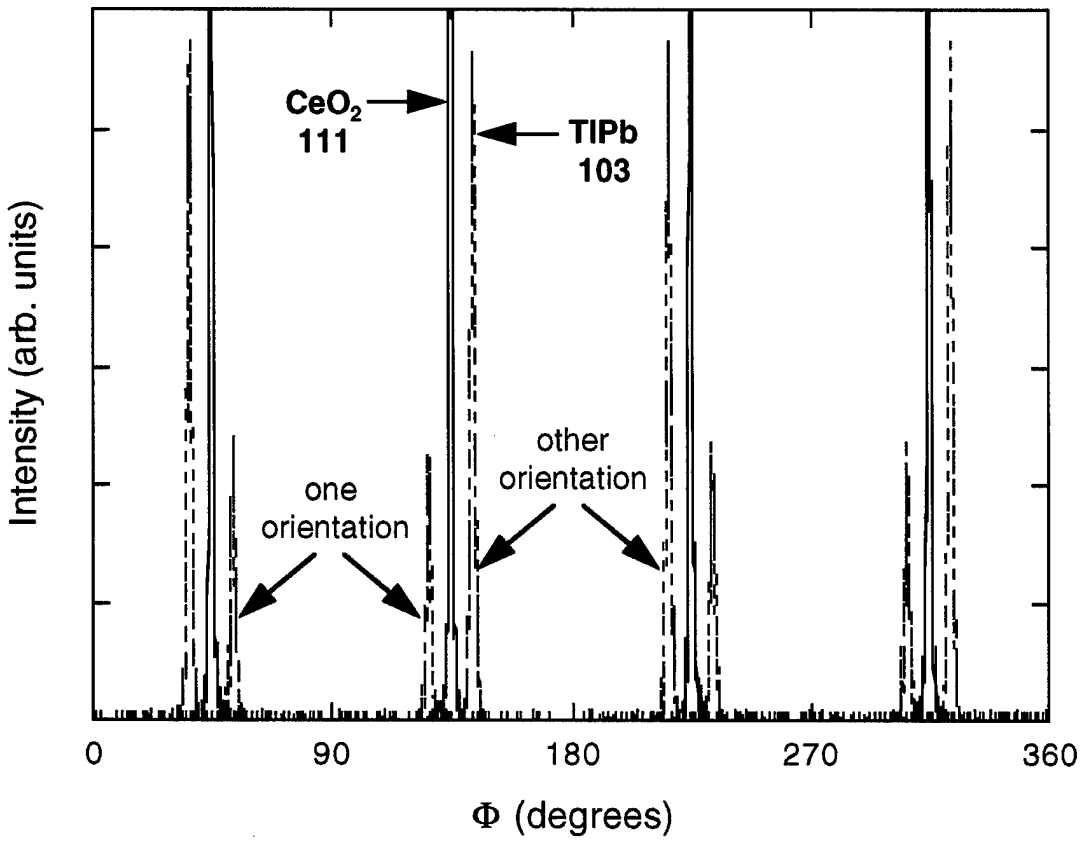


Figure 2.3.2.c: A phi scan through the 103 peaks of 110-oriented TlPb-1212 and the 111 peaks of 100-oriented $CeO_2$, grown sequentially on r-plane $Al_2O_3$. The two sets of reflections from the TlPb-1212 indicates that two in-plane crystallite orientations are present.

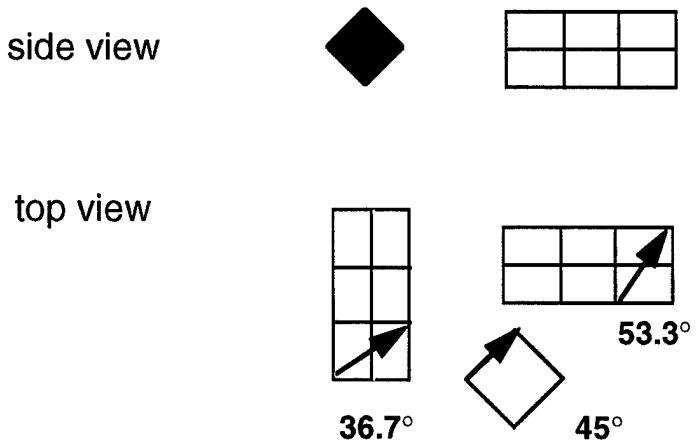


Figure 2.3.2.d: Schematic representation of the growth of TlPb-1212 in the 110 orientation showing the two possible in-plane orientations.

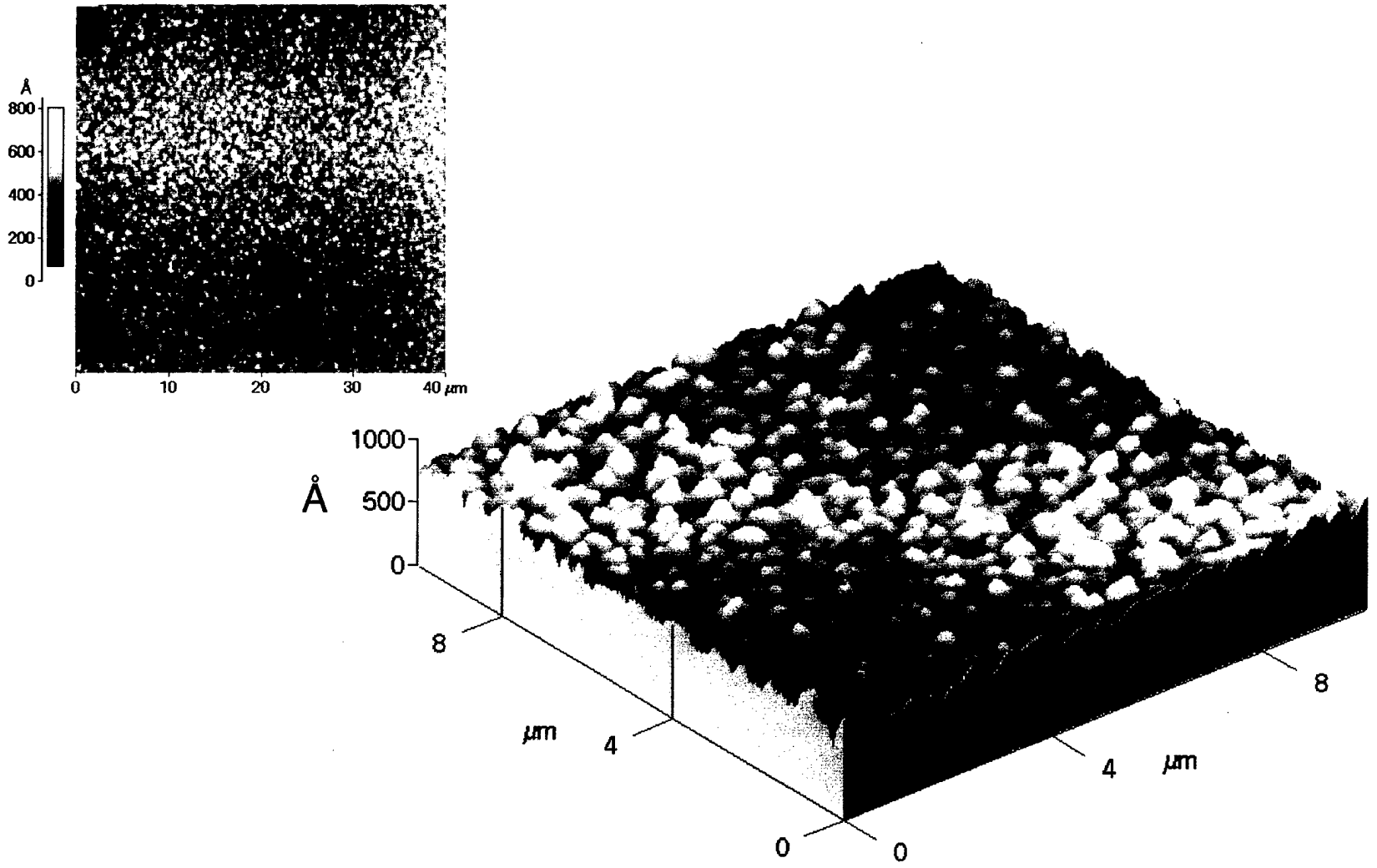


Figure 2.3.2.e: Atomic Force Microscopy of the surface of an 800 Å thick film of 110-oriented TlPb-1212 on $CeO_2$-buffered $Al_2O_3$.

### 2.3.3. *Future Directions*

We see three possible directions for future work in this area. One is to switch to a different radiative element with the hopes of reducing the thermal gradients so that $NdGaO_3$ wafers could be used. This could be successful, though there are likely to be continuing problems, perhaps at later stages of processing. Another possibility is to switch to a different buffer layer for sapphire, though the choices are certainly limited. Finally, one could try using MgO substrates with an appropriate choice of buffer layer.

## 2.4. *In situ* Growth Issues

### 2.4.1. Ex situ *Anneals*

One key learning was that *ex situ* furnace anneals without an external source of thallous oxide, do not work. The films experience significant thallium loss at high temperature, despite the one atmosphere oxygen ambient. At lower temperatures, where the thallium loss was not too severe, there was not significant improvement in the structure as measured by x-ray diffraction. Thus it appears likely that some level of thallous oxide partial pressure is extant in the *in situ* chamber during the normal anneal, even though the temperature of the thallium source is relatively low ($\approx$ 200°C).

### 2.4.2. *Recycling of Thallic Oxide*

Another lesson from this work is that one can't recycle material in the thallium source; it has to be fresh each time. We felt it would be advantageous to reuse the thallium oxide left-over from previous runs as this would lower costs and reduce toxic waste generation. We had also found that the thallium source is more stable when run with a mixture of fresh and reused material. We thought that since the thallous oxide rate is determined by the quartz crystal monitor, variations in surface area or the presence of some Sr, Ca and Cu deposits in the source might not matter. Unfortunately, we found that for a given set of conditions, better TlPb-1212 films were obtained when the thallium source was charged only with fresh $Tl_2O_3$ powder.

### 2.4.3. *Redesign of the Thallium Source*

We decided to redesign the thallium source because 1) the old source repeated failed due to oxidation of the pin-in-socket electrical leads, 2) the old thallium source exhibited oscillating behavior once the substrate rotation was introduced, and 3) the large thermal mass of the current source was thought to aggravate the wafer cracking problem discussed above.

A new thallium source, smaller and with lower thermal mass than the old one, was installed. It consists simply of a quartz bulb heat source surrounded by an insulated can and capped with a "boat" for source material. We note that after three months of operation, no deterioration or reaction of the quartz was observed. This has positive implications for future replacement of the Kanthal Super element by quartz bulbs in the radiant substrate heater. The electrical connections are heat sunk by a large copper block which can be water-cooled if need be.

The new thallium source was an improvement over the old one in that it maintains a stable rate regardless of the substrate rotation. It also heats up and cools down more quickly and is generally easier to control.

## 2.5. *In situ* Growth Results

### 2.5.1. *TlPb-1201 Thin Films*

We have demonstrated the growth of excellent normal metal TlPb-1201 films on neodymium gallate. A target of composition $Pb_{1.6}Sr_2Cu_{1.1}O_x$ was used. The substrate temperature and thallium rate were varied to optimize the TlPb-1201 growth as determined by x-ray diffraction. The films were grown on 2" single-side polished (SP) $NdGaO_3$ wafers. The best film was grown at a substrate temperature of 665 °C and a thallium rate of 2.2 Å/s (for a PbSrCuO deposition rate of ≈ 8.7 Å/min).

Figure 2.5.1.a shows an x-ray diffraction θ-2 θ scan of a 100 nm thick TlPb-1201 film on $NdGaO_3$. The film is nearly pure 001 oriented TlPb-1201 though there is a small peak from TlPb-1223 at 11.4°. Figure 2.5.1.b plots the width of the rocking curve of the TlPb-1201 004 peak measured at three points across the two inch wafer. The width of the peak decreased from 0.65° at the center to 0.34° at the edge of the wafer suggestive of a small temperature gradient during deposition.

The surface roughnesses of two TlPb-1201 films were measured by AFM. A 20 nm thick film had an RMS surface roughness of only 0.26 nm and a peak-to valley range of 2.1 nm (2 μm square). The smoothness of the film as measured by low angle x-ray scattering was in agreement with the AFM results. A 100 nm film, shown in Figure 2.5.1.c, had an RMS roughness and peak to valley range of 0.10 and 11.4 nm respectively. While there is room for improvement, these films should be smooth enough for making step SNS junctions.

### *2.5.2. TlPb-1212 Thin Films*

As mentioned in Section 2.3, some TlPb-1212 films were grown on two inch diameter $LaAlO_3$ substrates. We have been able to get good results across a 2" wafer in terms of both structure and transition temperature. The x-ray

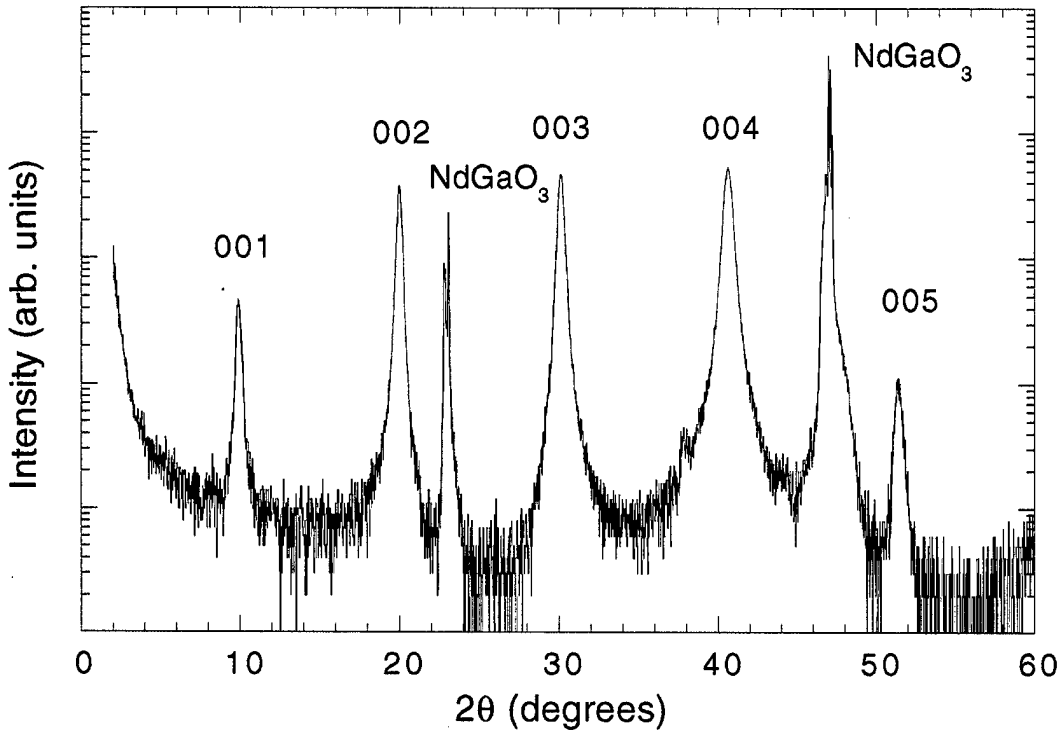


Figure 2.5.1.a: A θ-2θ scan of a 001-oriented film of TlPb-1201 on $NdGaO_3$.

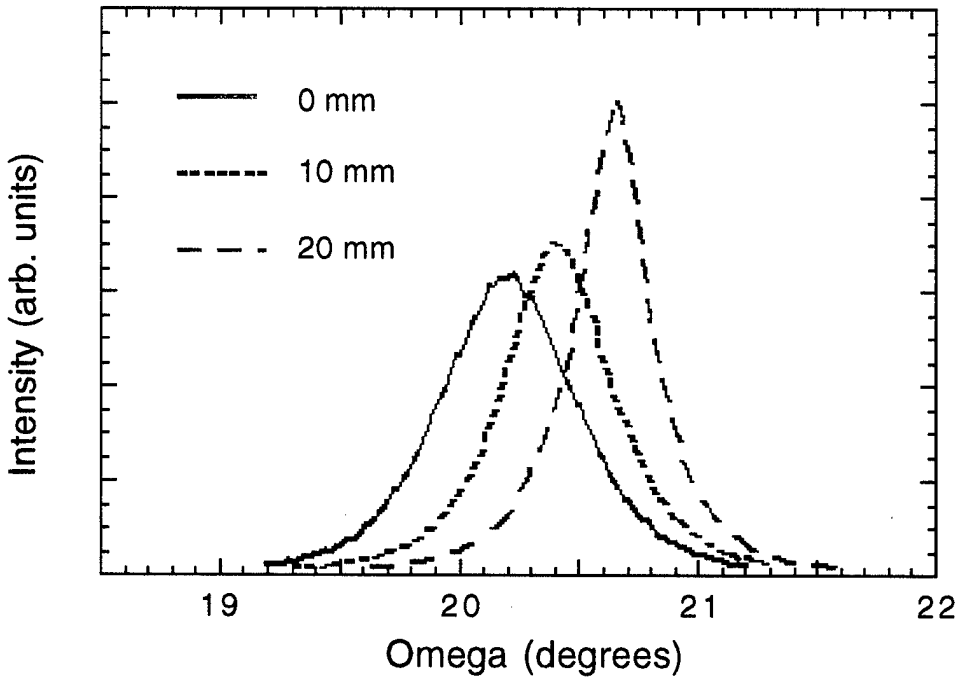


Figure 2.5.1.b: Variation across a 2" wafer of ω scans through the 004 reflection of a 001-oriented film of TlPb-1201 on NdGaO3.

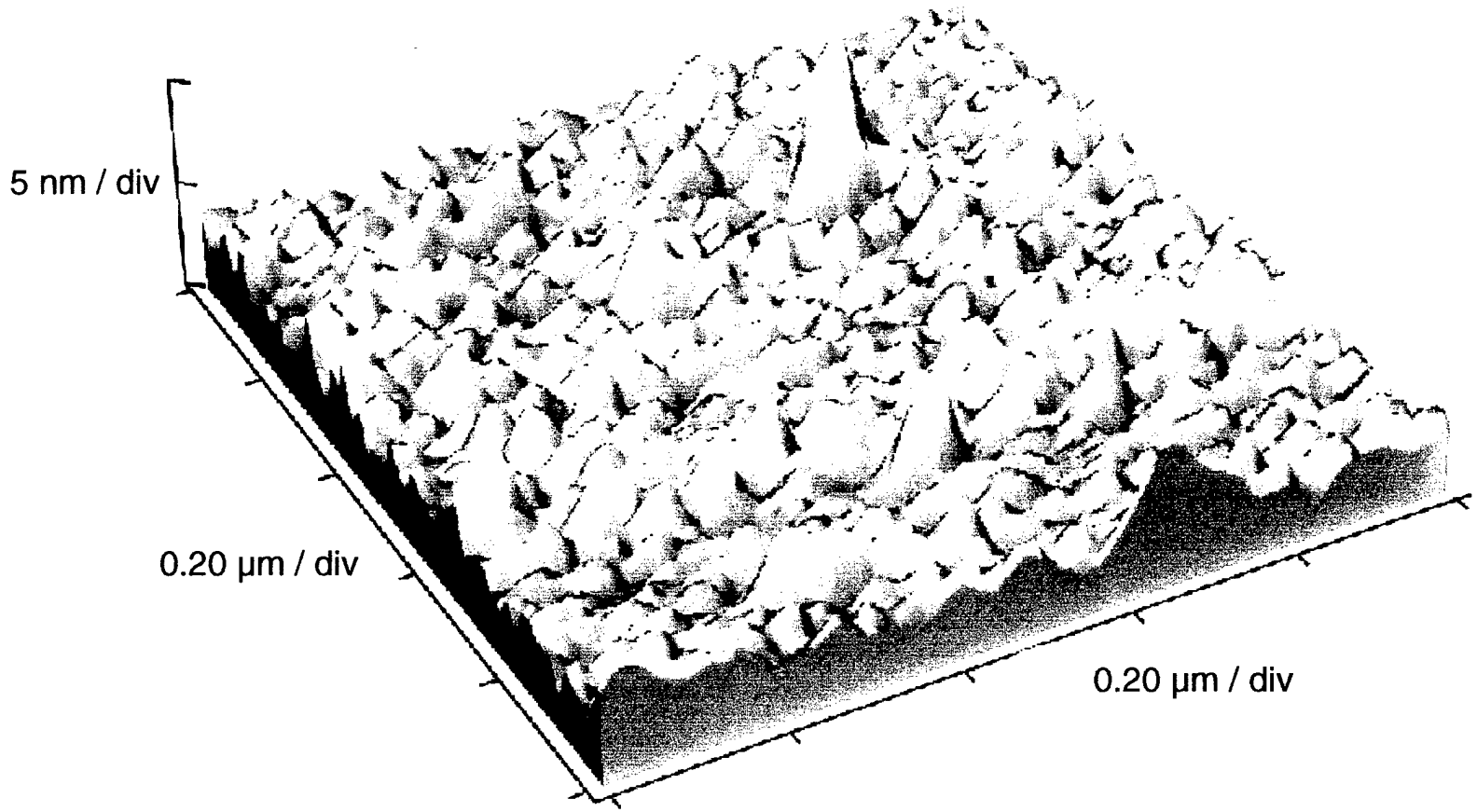


Figure 2.5.1.c: Atomic Force Mircroscopy of the surface of a 100 nm thick TlPb-1201 film on $LaAlO_3$.

diffraction θ-2 θ scan for a 70 nm TlPb-1212 film on $LaAlO_3$ is shown in Figure 2.5.2.a. The FWHM of the 005 rocking curve (Figure 2.5.2.b) varied from 0.61° at the center of the wafer to 0.42° at the edge. The transition temperature (Figure 2.5.2.c) was also uniform across the wafer, although at 84 K, it is lower than ideal for the 20% yttrium-doped composition. Unfortunately, the peak to valley surface roughness of this 70 nm TlPb-1212 is 50 nm, or 50% of the film thickness (Figure 2.5.2.d). The low transition temperature indicates that the growth conditions were not optimized and it is our expectation that the surface would improve with film quality.

### 2.5.3. *Compatibility of Cerium Oxide*

Prior to the present work, Face had successfully demonstrated the growth of $CeO_2$ on superconducting $TlBa_2(Ca_{0.75}Y_{0.25})Cu_2O_7$ (Tl-1212).[1] However, the growth of superconducting Tl-1212 on cerium oxide films had not been possible. In this work we were able to grow bilayers of both cerium oxide on TlPb-1212 and TlPb-1212 on $CeO_2$. In each case, both films were deposited during a single pump-down, as would occur during junction fabrication.

Figures 2.5.3.a and 2.5.3.b show x-ray data for $CeO_2$/TlPb-1212/$LaAlO_3$ and TlPb-1212/$CeO_2$/$NdGaO_3$ bilayer samples, respectively. The TlPb-1212 is c-axis

---

[1] Dean W. Face, Dennis J. Kountz, and Joseph P. Nestlerode, in *Advances in Superconductivity VI*, T. Fujita and Y. Shinohara, Eds. (Springer-Verlag: Tokyo, 1994), p. 863.

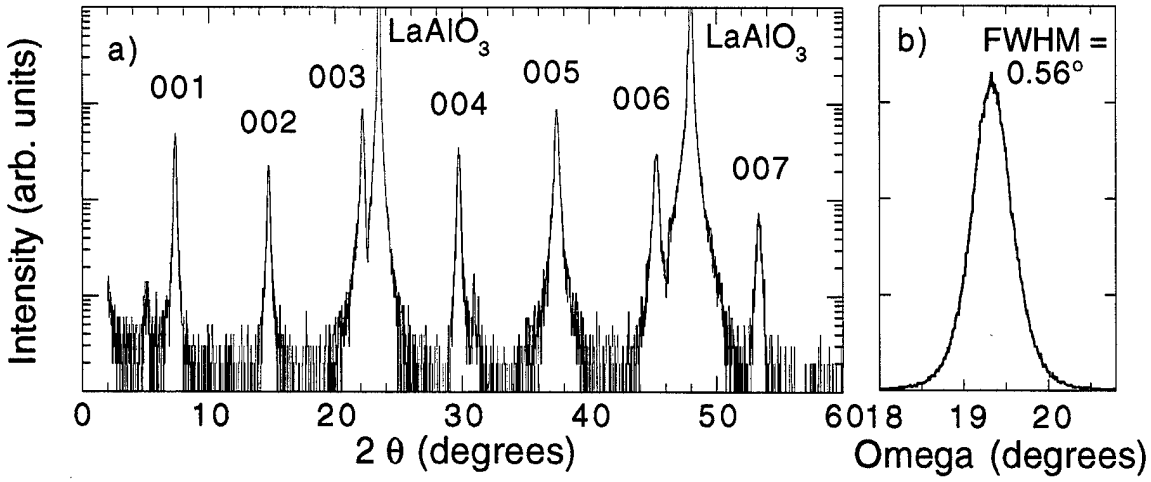


Figure 2.5.2.a) X-ray diffraction θ-2θ scan of a 70 nm thick film of TlPb-1212 on $LaAlO_3$. b) ω-scan through the 005 peak of the same film.

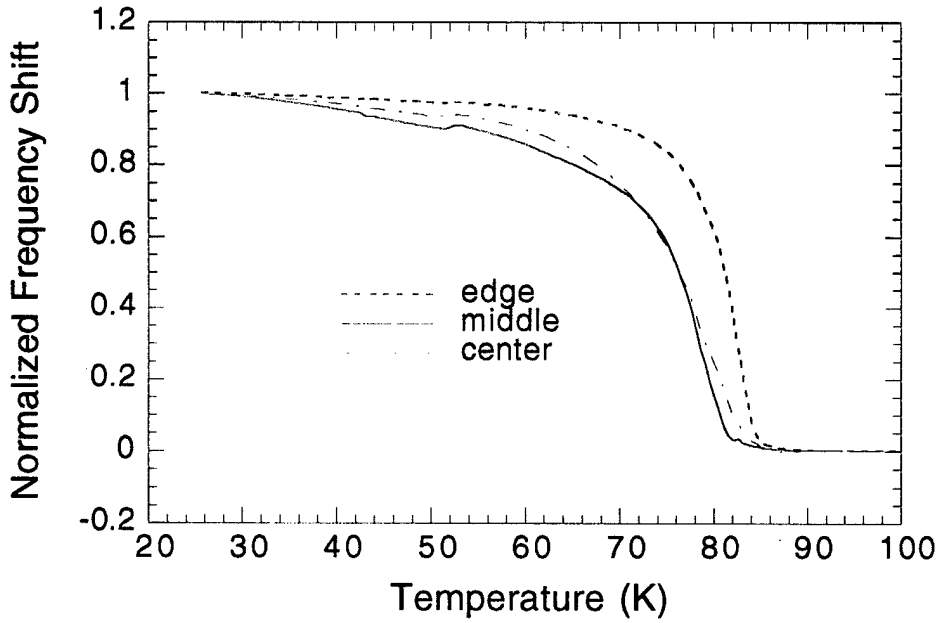


Figure 2.5.2.c: Inductive measurements of the transition temperature of a TlPb-1212 film across a full two inch $LaAlO_3$ wafer.

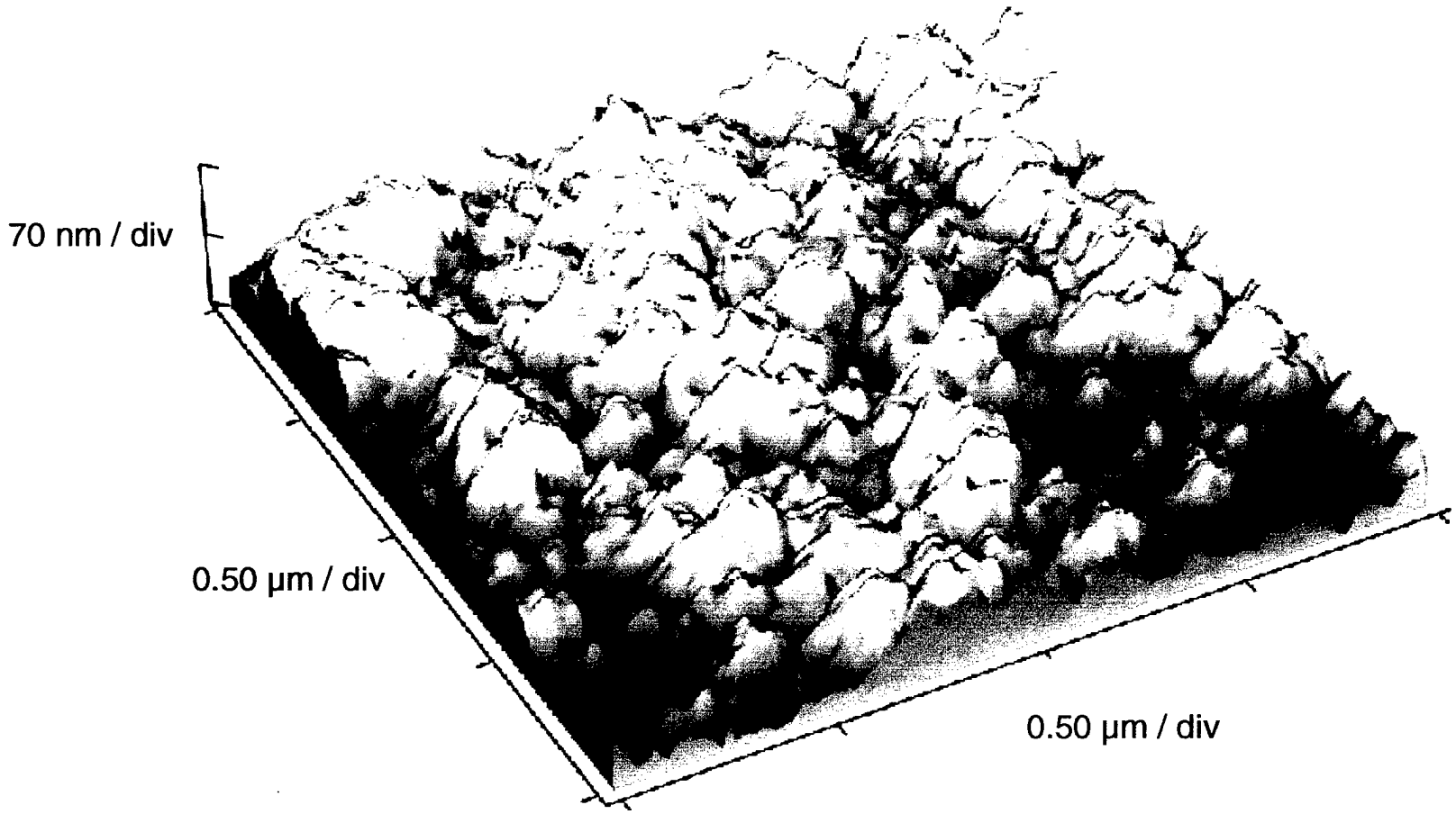


Figure 2.5.2.d: Atomic Force Microscopy of the surface of a 70 nm thick TlPb-1212 film on $LaAlO_3$.

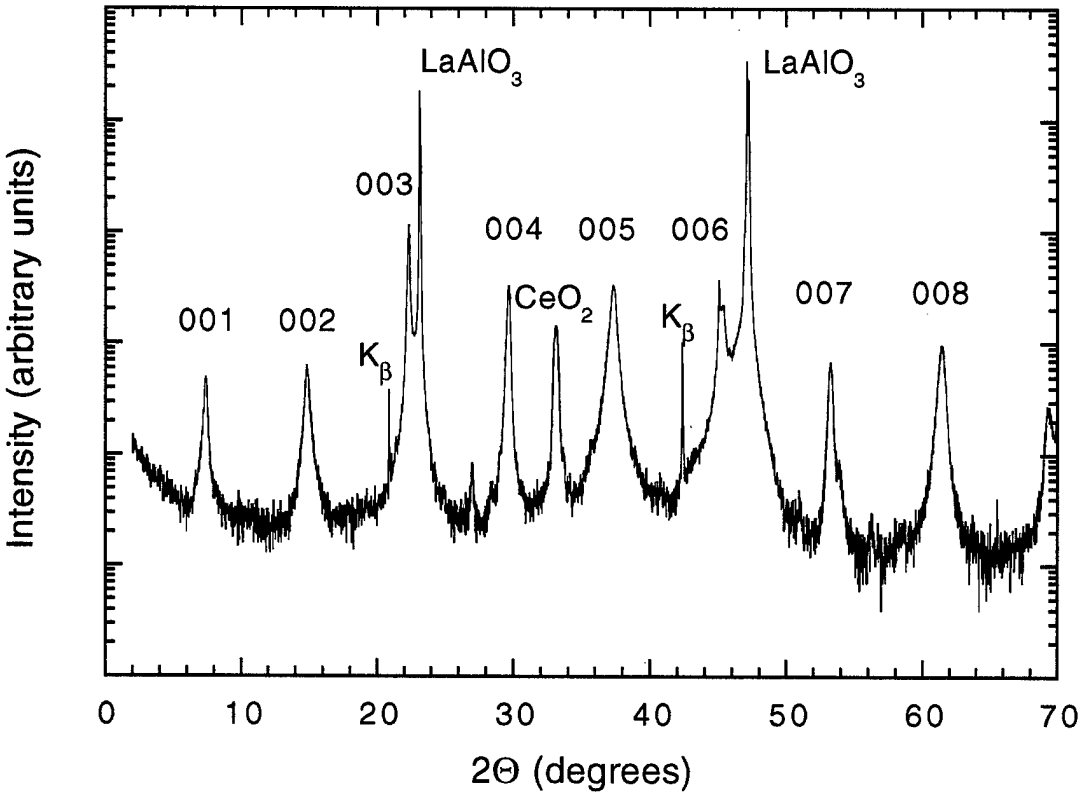


Figure 2.5.3.a: θ-2θ scan of a $CeO_2$ / TlPb-1212 bilayer on $LaAlO_3$.

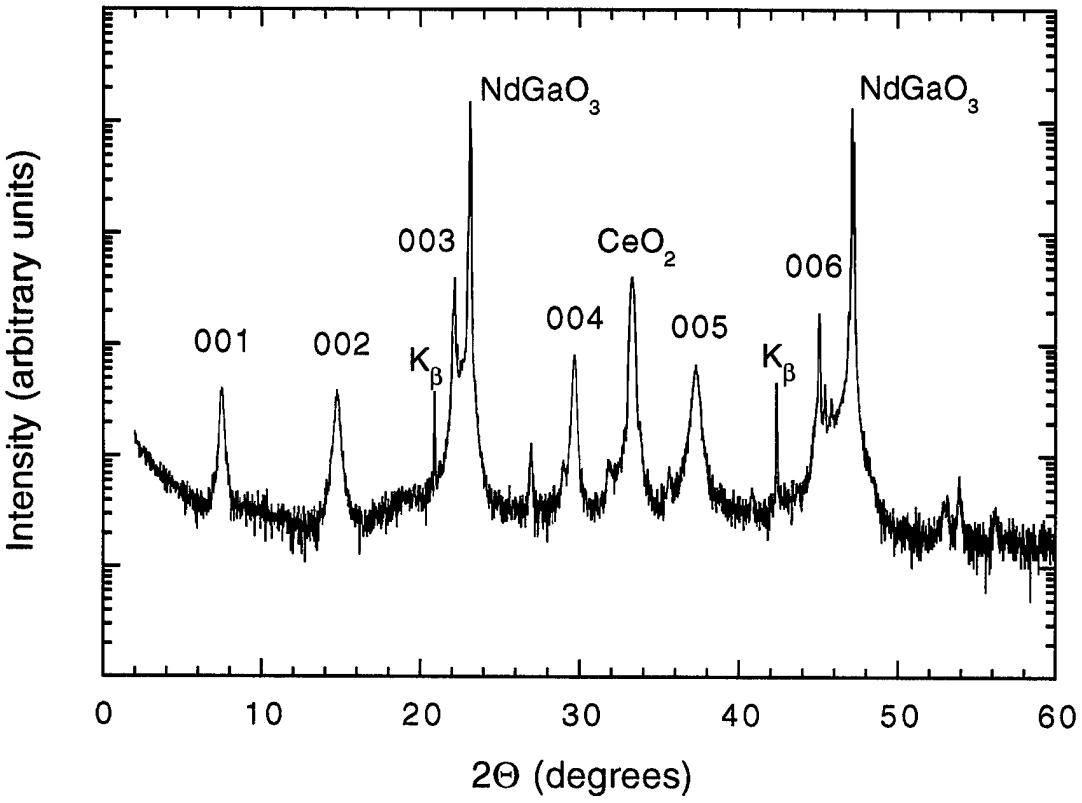


Figure 2.5.3.b: θ-2θ scan of a TlPb-1212 / $CeO_2$ bilayer on $NdGaO_3$.

oriented and the $CeO_2$ shows a single (100) orientation. There are some very small peaks due to second phase material in both samples. They are most likely due to a strontium cerate phase. If so, that would indicate some level of reaction between the $CeO_2$ and thallium lead film. That would not, however, pose a problem for the junction program given that the $CeO_2$ or TlPb-1212 overlayer is oriented properly. Most likely, a reaction occurred during the higher temperature anneal. In Figure 2.5.3.c we show inductive measurements of the superconducting transition temperatures of TlPb-1212 films in the two types of bilayer samples. While not optimal, the results are promising and show that CeO2 is compatible with the *in situ* growth process.

## 2.6. Thallium cuprate materials

### *2.6.1. Optimal Yttrium Dopant Level*

In our prior work on yttrium doped TlPb-1212, the yttrium doping level was set at 20% because studies of sintered ceramic pellets of TlPb-1212 had shown a maximum $T_c$ at that composition.[2] A comprehensive study of $T_c$ as a function of yttrium doping had not been made.

---

[2] J.M. Liang, R.S. Liu, Y.T. Huang, S.F. Wu, P.T. Wu, and L.J. Chen, Physica C **165**, 347 (1990).

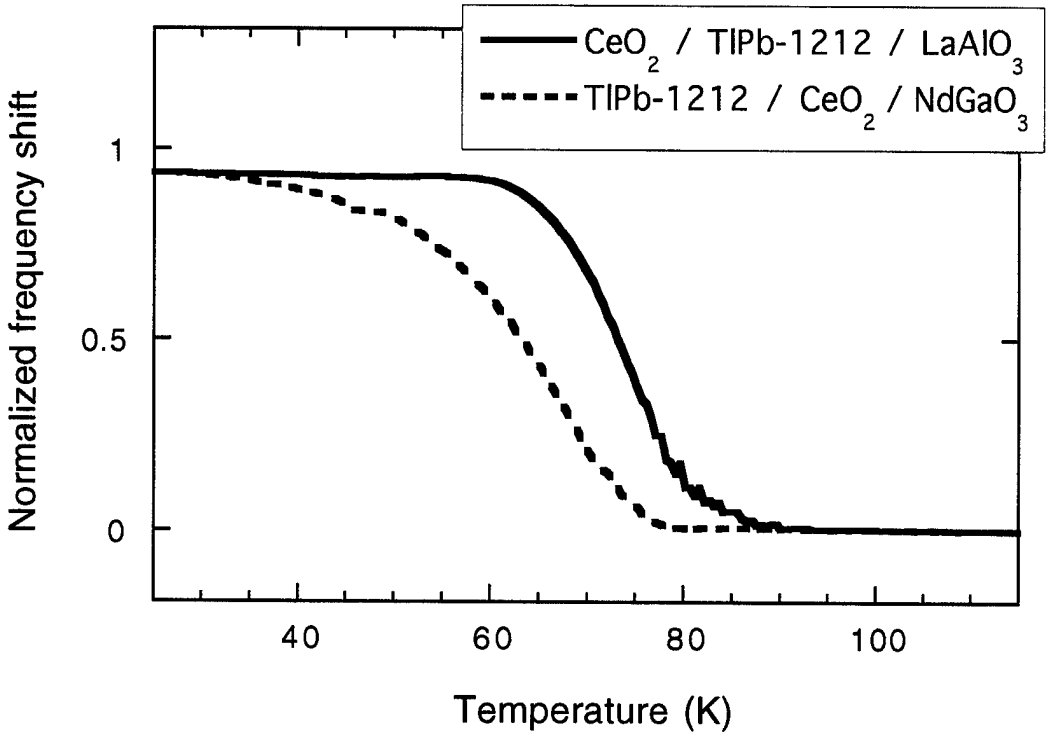


Figure 2.5.3.c: Inductive measurement of the transition temperature of TlPb-1212 in two bilayer structures.

We did two series of experiments designed to determine the optimal yttrium concentration for thin films of TlPb-1212 made by our *in situ* technique. It is not obvious that the optimal yttrium concentration is the same for the films as it is in the bulk. In TlPb-1212, as for any of the HTS materials, one must adjust the overall carrier concentration to get the maximum $T_c$. Doping with yttrium on the calcium site increases the carrier concentration, but so does increasing the lead to thallium ratio. In films, it is difficult to measure the thallium to lead ratio and therefore know how close it is to one. It therefore seemed prudent to measure the $T_c$ of films as a function of yttrium doping. First we made films using one target of composition $Pb_2Sr_2Ca_{0.8}Y_{0.2}Cu_{2.1}O_x$ and another of composition $Pb_2Sr_2Ca_{0.7}Y_{0.3}Cu_{2.1}O_x$. Using targets with different yttrium concentrations produced a composition spread across the substrate area. We then varied the growth conditions around the best known conditions for growth of the $(Tl,Pb)Sr_2Ca_{0.8}Y_{0.2}Cu_2O_7$ composition. We varied the substrate temperature ($T_s$) from 540 to 600°C and the $TlO_x$ rate from 24 to 29 Å/min.

For a second set of depositions, we used targets with compositions of $Pb_2Sr_2Ca_{0.8}Y_{0.2}Cu_{2.1}O_x$ and $Pb_{1.6}Sr_2Ca_{0.9}Y_{0.1}Cu_{2.1}O_x$. Based on the results from the first series, we performed depositions at a smaller set of conditions. The results are plotted in Figure 2.6.1.a for one $TlO_x$ rate and two substrate temperatures. The results at other conditions followed the same trend, namely that the $T_c$ is highest at twenty percent yttrium doping. One caveat to the above is that the targets with 10 and 30% yttrium doping were

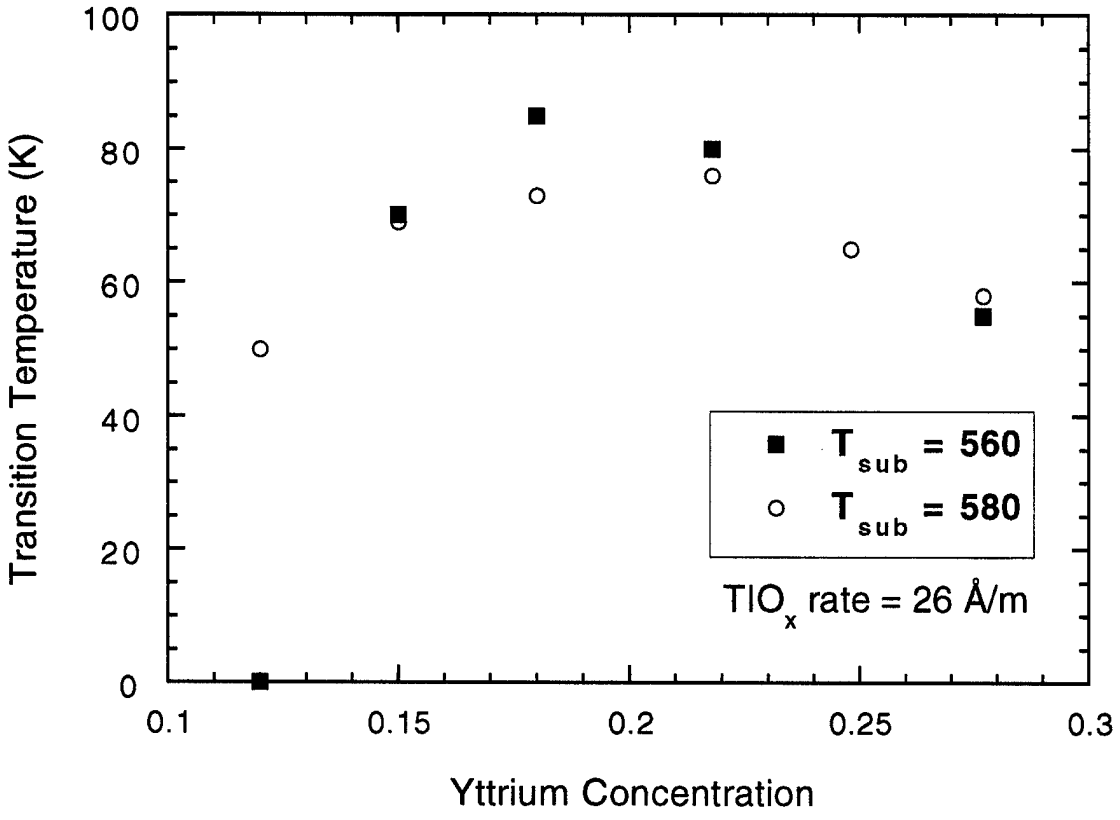


Figure 2.6.1.a: Transition temperature as a function of yttrium concentration in TlPb-1212 thin films.

contaminated with about 1% barium. It is not known what effect the small barium impurity may have had on the results.

### 2.6.2. *Potassium Doping*

We did not intentionally investigate the effects of potassium doping on thallium lead cuprates. Unfortunately however, we were at one point supplied with "99.999% pure" $Tl_2O_3$ which contained approximately 0.8% potassium. The potassium successfully competes for the thallium site in the 1212 structure. The result was that the x-ray diffraction patterns showed the 1212 structure, but the samples did not contain significant amounts of thallium or lead, as measured by Energy-Dispersive X-ray Analysis (EDX). These potassium doped samples were highly resistive and not superconducting.

### 2.6.3. *Electromigration Studies*

In our original proposal, we argued that "It is generally accepted that a primary source of the variability in SNS $YBa_2Cu_3O_7$ (YBCO) junctions is the presence of oxygen defect states in the YBCO near the junction. These defect sites are due to the high mobility of oxygen in YBCO. High oxygen mobility is also responsible for the time-dependent character of many junctions. The thallium cuprate superconductors have lower oxygen mobilities than YBCO, making them less susceptible to stress and more stable. Lower oxygen

mobilities may enable maintenance of the superconducting order parameter to the HTS surface, leading to higher $I_cR_n$ products."

While the oxygen in TlPb-1212 appears to be more stable against thermal treatment, the challenge to oxygen stability in a junction might be more likely to come from current flow. We provided samples of our TlPb-1212 films to Jason Sydow, a graduate student of Dr. Robert Buhrman at Cornell University, for investigation of the stability of TlPb-1212 to electromigration. The following discussion of the electromigration experiment paraphrases and borrows directly from materials provided by Sydow.

Electromigration consists of the application of an electrical bias with a current density of 1-5 MA/cm$^2$ to a thin film microstructure. This process is generally conducted in 1 atm. of He and at room temperature, although there is some ohmic heating of the microstructure. The current bias induces long range migration of the positively charged oxygen vacancies towards the negative electrode, if those vacancies are sufficiently mobile.

Thin TlPb-1212 films were patterned into microstructures by optical lithography and argon ion beam milling. The data presented herein were taken on a 3 x 50 μm bridge patterned in a 60 nm thick film. Ag/Au contact pads were thermally deposited after an in-situ 90% argon and 10% oxygen ion beam clean of the contact pad area defined by photoresist.

Figure 2.6.3.a shows the room temperature resistance of a TlPb-1212 microbridge as a function of time as various bias currents are applied. Between different levels of bias current, a small sensing current was applied in order to observe the effect of the previous bias current on the sample resistivity. We see that after application of the 3 mA bias current (1.67 $MA/cm^2$), the resistivity of the bridge starts to decrease. Figure 2.6.3.b shows that the transition temperature also decreases with increased bias current during electromigration. This indicates that the doping of the TlPb-1212 material is being changed by the electromigration process; it is being overdoped.

The bias current required to alter TlPb-1212 is comparable to that required for YBCO. Thus the mobility of oxygen in this material does not appear to be any more stable than any other HTS material, at least with respect to electromigration. The projected benefits of reduced oxygen mobility on junction stability are therefore unlikely to materialize.

## 3. Dissemination of Results

The data generated during this program have been, and will continue to be, widely disseminated via presentations at technical meetings and publications in peer reviewed journals. Dr. Myers was invited to give talks on *in situ* deposition of thallium lead cuprates at the American Ceramic Society Annual meeting and the International Workshop on Tl and Hg Based

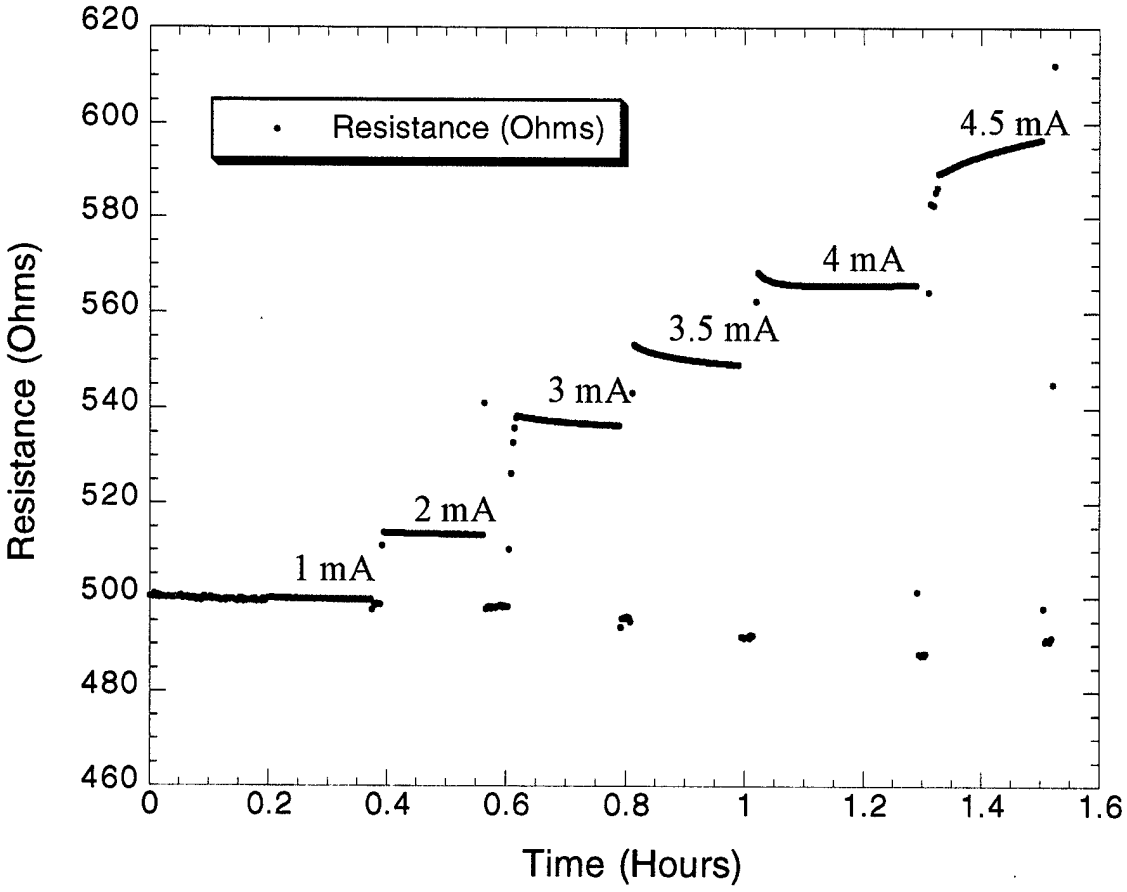


Figure 2.6.3.a: Electromigration of a TlPb-1212 microbridge (3 μm wide, 60 nm thick and 50 μm long) at increasing bias levels. Figure courtesy of Jason Sydow, Cornell University.

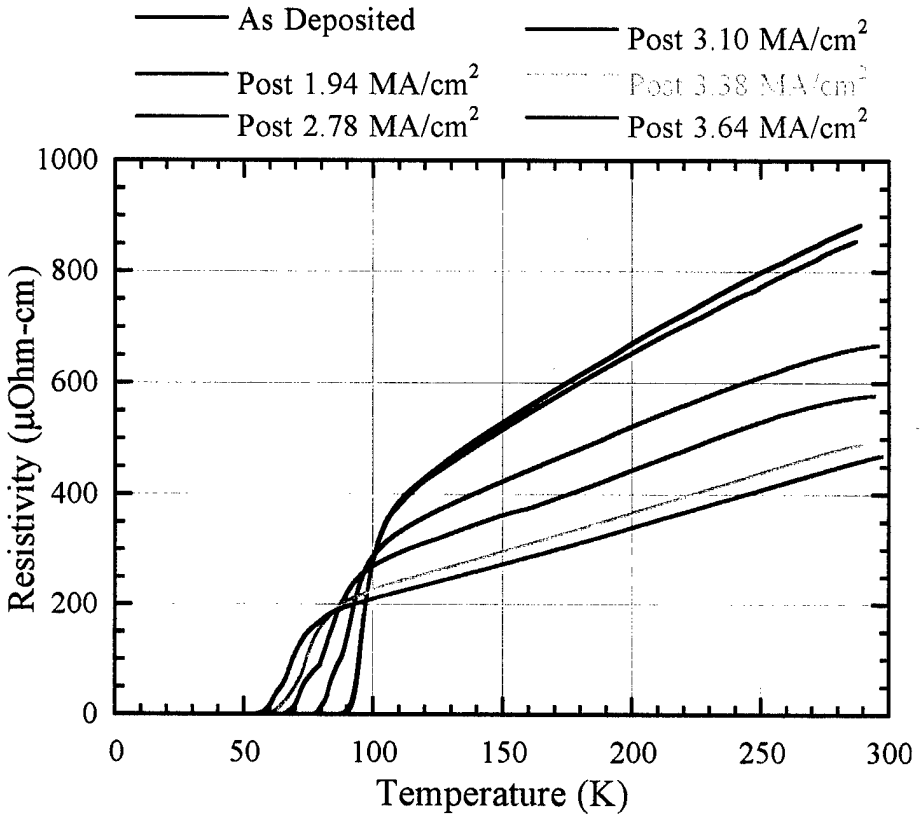


Figure 2.6.3.b: Resistivity as a function of temperature for a TlPb-1212 microbridge after electromigration at increasing bias levels. Figure courtesy of Jason Sydow, Cornell University.

Superconducting Materials, both in May, 1997. The title of her presentations was "Full Wafer *In situ* Deposition of Thallium Lead Cuprates." In addition, Dr. Myers gave a talk at the 1996 American Physical Society March Meeting entitled, "Thallium Tantalate for Multilayer Tl-Cuprate Devices" and presented a poster entitled, "*In Situ* Deposition of TlPb-1212 on 2" Sapphire Wafers," at the 1997 Fall Meeting of the Materials Research Society.

The article, "Full Wafer *In situ* Deposition of Thallium Lead Cuprates" by K. E. Myers and Lijie Bao appeared earlier this year in the Journal of Superconductivity (vol. 11, issue 1, p. 129-132, 1998). That article is included in this report as Appendix A. A second article, on the growth of 110-oriented TlPb-1212 on cerium oxide-buffered sapphire wafers, is in preparation.

**4. Financial and Program Management**

The program, managed by Dr. Myers, was kept within budget despite several serious equipment failures and technical difficulties. Unexpected equipment failures included the premature failure of the old substrate heater, as well as the failure of two elements for the new heater. The thallium source had to be re-engineered as its short-comings started to negatively impact progress. Finally, the continuing problem of wafer breakage represented a cost drain, particularly given the high cost of neodymium gallate wafers.

## 5. Deliverables

With the submission of this Final Report, all Deliverables under Contract # N00014-96-C-2005 will have been meet. These deliverables include with the Monthly Financial Reports (Data item # A001), Informal Monthly Progress Reports (Data item # A002), First Interim Report (Data item # A003), Second Interim Report (Data item # A004), Draft Version of Final Report (Data item # A005), Final Report (Data item # A006), and Viewgraphs and Visual Materials as requested (Data item # A007).

## 6. Conclusions

The Development of High Temperature Superconducting Josephson Junction Device Technology program was successful in generating useful knowledge about thallium cuprate materials, photoresist reflow processing, and radiant heater technology though it did not lead to a new junction technology. Among the achievements of this program was the *in situ* fabrication of both (Tl,Pb)$Sr_2CuO_5$ and (Tl,Pb)$Sr_2Ca_{1-x}Y_xCu_2O_7$ films on full two inch wafers. These films were uniform in properties and had quite smooth surfaces as predicted. We were also able to grow bilayers of TlPb-1212 on $CeO_2$, and vice versa, and thus qualify cerium oxide as compatible with the *in situ* growth process and suitable in a thallium-based multilayer technology. In addition, this project resulted in the first-ever epitaxial thallium cuprate films with copper oxide

sheets oriented out of the plane of the film: 110 oriented TlPb-1212 on cerium oxide-buffered sapphire.

A key learning in the area of photoresist reflow processing was that these processes are clearly feature size and shape dependent This can be a problem for research efforts which typically rely on junction parameters scaling with area in order to prove tunneling. We found the use of Kanthal Super elements in radiative heaters expensive and unreliable.

The DuPont program has determined that the standard HTS substrates, neodymium gallate, cerium oxide-buffered sapphire, and lanthanum aluminate, are not ideal for an *in situ* thallium cuprate junction technology. Neodymium gallate substrates do not have sufficient thermal conductivity or strength. Growth on cerium oxide buffered sapphire results in non c-axis oriented films and of, course, lanthanum aluminate has twins which interfere with multilayer processing.

Moreover, we have found that (Tl,Pb)$Sr_2Ca_{1-x}Y_xCu_2O_7$ can be as susceptible to electromigration as $YBa_2Cu_3O_7$. The potentially greater stability of TlPb-1212 was considered to be one of the key benefits of developing this new technology. The development of stable, reproducible multilayer SNS junctions is thus no more likely using thallium lead cuprates as using other HTS materials systems.

DuPont has decided not to pursue further a multilayer thallium cuprate junction technology at this time. Several technical hurdles remain which, to overcome, would require new ideas, new materials, and, most importantly, a significant financial commitment. Naturally, we remain interested in superconducting digital electronics development, and will continue to monitor progress in this area. We would welcome any new idea or material that could push the technology forward and justify additional investment. However, because the choice of substrate, superconductor, and normal metal are all important in determining the properties of junctions, any future work should consider a total materials systems development approach.

## 7. Appendix A

"Full Wafer *In situ* Deposition of Thallium Lead Cuprates" by K. E. Myers and Lijie Bao, *Journal of Superconductivity*, volume 11, issue 1, p. 129-132, January, 1998.

Invited Paper

# *In situ* deposition of thallium-containing oxides

K. E. Myers

DuPont CR&D, Experimental Station E304/C110
Wilmington, DE 19880-0304

## ABSTRACT

The number and variety of thallium based materials that can be made by *in situ* methods have grown consistently since the first report of successful thallium cuprate deposition by Face and Nestlerode in 1992. Processes for the deposition of superconductors, normal metals, and insulators have been developed. Most work to date has been done on the Tl-1212 phases, $TlBa_2CaCu_2O_7$ and $(Tl,Pb)Sr_2CaCu_2O_7$. Recently however, the *in situ* thallium technique has been extended to other materials. For example, epitaxial thin films of thallium tantalate, an insulator of the pyrochlore structure and a potential buffer layer for thallium cuprate films, have been grown. Multilayers, important in the fabrication of Josephson junctions, have been demonstrated with the thallium lead cuprates. This paper reviews progress in the area of *in situ* thallium deposition technology which will make more complex thallium cuprate multilayer structures and devices possible.

Keywords: superconductors, thallium cuprates, thin films, *in situ* deposition, TlBaCaCuO, TlPbSrCaCuO, $Tl_2Ta_2O_6$

## 1. INTRODUCTION

The first reports of thallium cuprate thin films were published in 1988, the same year this interesting class of High Temperature Superconductors (HTS) was discovered by Sheng and Hermann.[1] However, the development of thallium cuprate thin film technology was slow, due in part to the high volatility of thallous oxide, which greatly complicates film growth. Thin films of $Tl_2Ba_2CaCu_2O_8$ (TlBa-2212) became commercially available in 1991. High quality TlBa-2212 films have transition temperatures ($T_c$) of 105 K and surface resistances ($R_s$) as low as 140 μΩ at 10 GHz and 77 K. Because of their excellent characteristics, these thin films are being used in a variety of prototype microwave devices such as stabilized local oscillators, low-loss delay lines, and high power filters.[2]

Typically, commercial thallium cuprate films are made by a two-step, *ex situ* process. The first step is the deposition of a "precursor film," an amorphous, mixed oxide film, which may or may not contain thallium. The precursor film is then annealed under a high thallous oxide vapor pressure to form the crystalline superconducting phase. Precursor films can be deposited on both sides of the substrate resulting in double-sided films, ideal for microwave devices with ground planes.

Some applications however, such as Josephson Junctions (JJs) and Superconducting Quantum Interference Devices (SQUIDs), require more complex multilayer structures. Fabrication of multilayer structures is not feasible with a two-step process due to the high anneal temperatures (usually 840 - 900 °C) required in the thallination process. A process which enables thallium to diffuse several thousand Ångstroms into a precursor film will likely allow diffusion between layers. Thus two-step, *ex situ* processes are generally limited to the fabrication of single layers.

*In situ* deposition, such as that used in the deposition of $YBa_2Cu_3O_7$ (YBCO), is easily extended to the fabrication of multilayers. Indeed, complex multilayer devices and circuits have been made with YBCO in combination with a host of other perovskites: $SrTiO_3$, $PrBa_2Cu_3O_7$, and $CaRuO_3$, to name a few.[3] Despite the large resource investment in this technology, HTS JJs are not yet suitable for large-scale commercial applications. Low yields and non-reproducibility are universally recognized problems. Junctions of certain geometries, including those using sub-micron line widths or regions of suppressed superconductivity, have unstable characteristics. While significant progress has been made, there is still a need for increased junction performance.

It is generally accepted that a primary source of the variability in YBCO junctions is the presence of oxygen defect states in the YBCO near the junction. These defect sites are due to the high mobility of oxygen in YBCO. High oxygen mobility may



0-8194-2071-9/96/$6.00

also be responsible for the deterioration with time of many YBCO junctions. Certain thallium cuprate superconductors have lower oxygen mobilities than YBCO, making them less susceptible to oxygen defects at grain boundaries and more stable. Lower oxygen mobilities may enable preservation of the superconductivity all the way to the HTS interface in junction structures, leading to higher $I_cR_n$ values, the product of the critical current and normal state resistance of the junction and an important measure of junction performance. Thus, many of the problems plaguing YBCO JJ development may be avoided or reduced in the development of thallium cuprate Josephson Junctions.

In the absence of an *in situ* thallium deposition process, work on thallium cuprate Josephson Junctions was limited to single layer structures. Most of these JJs were grain-boundary junctions.[4,5] Grain boundary junctions are of limited commercial interest because the geometry of the actual junction cannot be controlled, hence the junction characteristics are irreproducible. Note however that high $I_cR_n$ products, up to 300 μV at 77 K, have been observed for thallium cuprate junctions.[6] Intrinsic stacked junctions have also shown interesting properties,[7] but again, are of limited commercial interest.

Multilayer ramp-type Superconductor/Normal Metal/Superconductor (SNS) junctions should have more controllable and reproducible characteristics. HTS ramp-type junctions were first introduced by Laibowitz and co-workers at IBM.[8] The SNS ramp-type junctions made today typically consist of a Normal metal/Superconductor epitaxial bilayer grown over a shallow ramp milled into a lower Superconductor layer. What makes the ramp-edge junction particularly attractive is that it has, in principle, a very controllable geometry. One can vary the normal metal thickness down to tens of Ångstroms, allowing one to tailor the critical current and resistance of the junctions to suit a particular application. *In situ* deposition of thallium cuprates will allow such structures to be made with the thallium cuprates.

The high volatility of thallous oxide,[9] discussed in the next section, complicates thallium thin film growth. Face and Nestlerode first demonstrated the *in situ* growth of superconducting thallium cuprate thin films using off-axis sputtering in the presence of thermally-generated thallous oxide vapor.[10] They were able to grow very smooth, epitaxial films of $TlBa_2CaCu_2O_7$ (TlBa-1212) on $LaAlO_3$, $NdGaO_3$ and $CeO_2$-buffered sapphire. By "*in situ*" I here refer to processes in which the material is fully superconducting when removed from the deposition chamber *and* in which the crystal structure is formed during growth. A two-step process, i.e. precursor deposition and thallination, carried out inside a single chamber is sometimes also referred to as an *in situ* process, which is technically correct. However, the film growth process is essentially the same as the *ex situ* process. The film growth process defined in this paper as "*in situ*" is quite different, and the film properties reflect that difference in growth mode.

Face and Nestlerode later reported the deposition of bilayer films of $CeO_2$ on yttrium doped TlBa-1212.[11] Continued work with the same technology led to the fabrication of $(Tl,Pb)Sr_2CaCu_2O_7$, $(Tl,Pb)Sr_2CuO_5$, and trilayer structures of the thallium lead cuprates.[12,13] Recently, Reschauer *et al.* reported the *in situ* deposition of $TlBa_2Ca_2Cu_3O_9$, the first of the three $Cu\text{-}O_2$ sheet materials to be made by an *in situ* technique.[14] In this paper, progress that has been made in the area of *in situ* thallium deposition technology is reviewed. Preliminary results on the deposition of insulating thallium tantalate, $Tl_2Ta_2O_6$, are also presented. The growth of this material is somewhat different from that of the cuprates and demonstrates the versatility of *in situ* thallium deposition techniques.

## 2. THE INFLUENCE OF $Tl_2O$ VAPOR PRESSURE

The main difficulty in the vapor phase deposition of thallium cuprate thin films is the high vapor pressure of thallous (I) oxide, $Tl_2O$. Work by Aselage and coworkers[15,16] and Holstein[9,17] in recent years has lead to a good working phase diagram of the Tl-O system. There appear to be three condensed phases, $Tl_2O_3$, $Tl_4O_3$, and $Tl_2O$, relevant to the fabrication of thallium-containing oxides. Thallic (III) oxide, $Tl_2O_3$, is a stable solid at ambient conditions. $Tl_2O_3$ decomposes to $Tl_4O_3$ at about 450 °C under the low oxygen partial pressures ($P_{O2}$) relevant to vapor phase deposition (10 - 100 mtorr). $Tl_4O_3$ decomposes to condensed $Tl_2O$ at lower $P_{O2}$. Of these thallium oxides, only $Tl_2O$, is stable in the gas phase. The thallous oxide partial pressure ($P_{Tl2O}$) depends strongly on oxygen partial pressure: $P_{Tl2O}$ is lower at high $P_{O2}$ and vice versa. Elemental thallium and TlO are also volatile, but are found at much lower partial pressures than $Tl_2O$ under the temperature and oxygen partial pressures ($P_{O2}$) conditions of interest. The reader is referred to Reference 9 for a more thorough treatment.

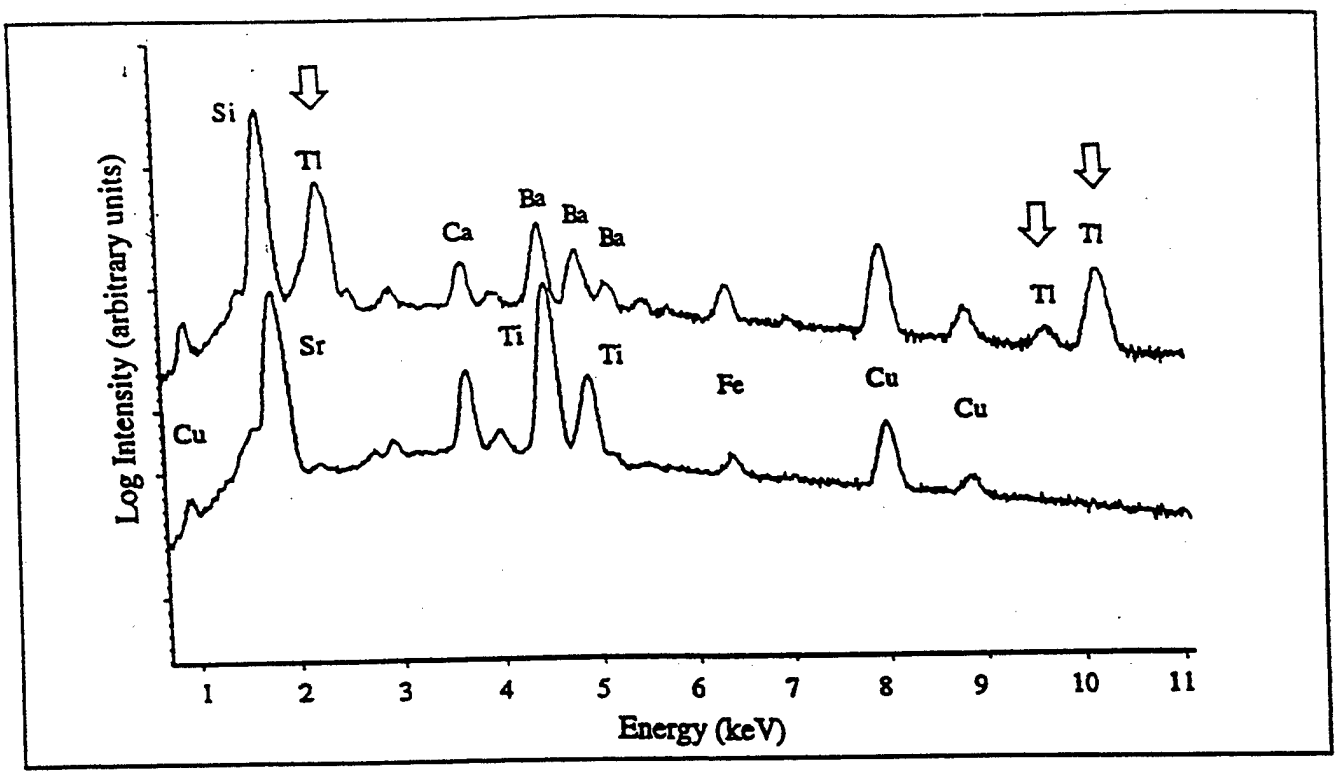


Figure 1: X-ray fluorescence data for films sputter-deposited from a TlBa-2212 target. The upper curve is for a sample deposited at room temperature (on silicon) and the lower curve is for a film deposited at Ts = 700 °C (on $SrTiO_3$). The arrows mark thallium peaks.

The result of the high volatility of thallous oxide is shown clearly in Figure 1. Energy Dispersive X-ray fluorescence (EDX) was used to measure the composition of films sputter-deposited from a stoichiometric $Tl_2Ba_2CaCu_2O_8$ (TlBa-2212) target at substrate temperatures ($T_s$) of 30 and 700 °C. Thallium is present in the film deposited at low temperature, but is not detectable in that deposited at high temperature. Both films were deposited in a mixture of 5% $O_2$ in Ar at 50 mtorr and applying 100 W of RF power to a 3" diameter magnetron sputter gun in the off-axis geometry.

Consideration of the partial pressure of $Tl_2O$ as a function of temperature and $P_{O2}$ is useful in evaluating deposition conditions for the thallium cuprates. Ideally, one would like to know the partial pressure of $Tl_2O$ over the thallium cuprate phase one intends to grow. Unfortunately, such data has not yet been collected for most experimental conditions. Aselage has collected data on the stability of several different superconducting phases at 880 °C and $P_{O2}$ = 0.8 atm and at 845 °C and $P_{O2}$ = .08 atm.[16] For those conditions, the $P_{Tl2O}$ required to stabilize the double Tl-O layer cuprates was between $5 \times 10^{-3}$ and $1.4 \times 10^{-2}$ atm. Comparing that to Holstein's data for $P_{Tl2O}$ over the condensed thallium oxides, one finds that the partial pressure of $Tl_2O$ over the double Tl-O layer cuprates is 10 to 100 times lower, for the conditions given. For the single Tl-O layer compounds, Aselage found that the $P_{Tl2O}$ required to form these phases is strongly dependent on $P_{O2}$, and lower than that for the double T-O cuprates. In section 4.2, estimates of the partial pressure of $Tl_2O$ over TlBa-1212 or TlPb-1212 during *in situ* growth are made. It is found that $P_{Tl2O}$ over the single Tl-O layer cuprates is $10^3$ to $10^4$ times lower than that over $TlO_x$ for the growth conditions used (580 °C and $P_{O2} = 1.3 \times 10^{-4}$ atm.).

An estimate of the thallous oxide partial pressure necessary to grow TlBa-2212 under the conditions particular to the experiment of Figure 1 can be made. Using the thermodynamic data of Reference 9, the equilibrium $P_{Tl2O}$ over condensed $TlO_x$ is calculated to be about 10 torr for the high temperature deposition. Reducing this by two orders of magnitude to account for the different $P_{Tl2O}$ over TlBa-2212 as compared to the oxides, the required $P_{Tl2O}$ is still 100 mtorr. Obviously, the thallous oxide generated from the sputter target would be insufficient to provide such a high $Tl_2O$ partial pressure. Most of

the thallium liberated in the sputtering process would have remained in the vapor phase until it was pumped away or condensed on the cold chamber walls.

As noted earlier, there is an inverse relationship between $P_{Tl2O}$ and $P_{O2}$ over a $TlO_x$ source. The relationship between $P_{Tl2O}$ and $P_{O2}$ over each of the thallium cuprates can be determined from equilibrium expression for the formation or decomposition of the phase, assuming one knows the reactants. Face and Nestlerode have given such an expression for TlBa-1212:[10]

$$2\,TlBa_2CaCu_2O_7\,(s) \xleftrightarrow{K} 4\,BaCuO_2\,(s) + 2\,CaO\,(s) + Tl_2O(g) + (3/2)\,O_2\,(g) \qquad (1)$$

The equilibrium constant K for this reaction is then:

$$K = \exp\left(\frac{-\Delta G^0}{RT}\right) = (P_{Tl2O})(P_{O2})^{3/2} \qquad (2)$$

where $\Delta G^0$ is the Gibbs free energy for the reaction and R is the Universal gas constant. From Equations 1 and 2, it is seen that at a given temperature, increasing the oxygen partial pressure reduces the $P_{Tl2O}$ that must be present for TlBa-1212 to be stable. Alternately, lowering the temperature lowers the required $P_{Tl2O}$ at a given $P_{O2}$. These relationships have been confirmed qualitatively for the TlBa-1212 phase.[11] For TlBa-2212, similar equations can be written; the $P_{O2}$ exponent in the expression for K would be 1/2 instead of 3/2. There may well be multiple reactions relevant to this system however, and it is not clear that this is indeed the correct equilibrium expression to consider.[17] On the other hand, the sign of the relationships between $P_{Tl2O}$, $P_{O2}$ and temperature are likely to be correct.

## 3. DEPOSITION PROCESS

In this section the sputter deposition apparatus used by the DuPont group for *in situ* deposition of thallium-containing oxides is described. General aspects of the deposition process are also given. The specifics for each material are noted in Section 4. *In situ* deposition of TlBa-1223 done at the Universität Regensburg utilized a different apparatus and process, specifically pulsed laser deposition and thermal evaporation of thallous oxide, which will be discussed in Section 4.3.

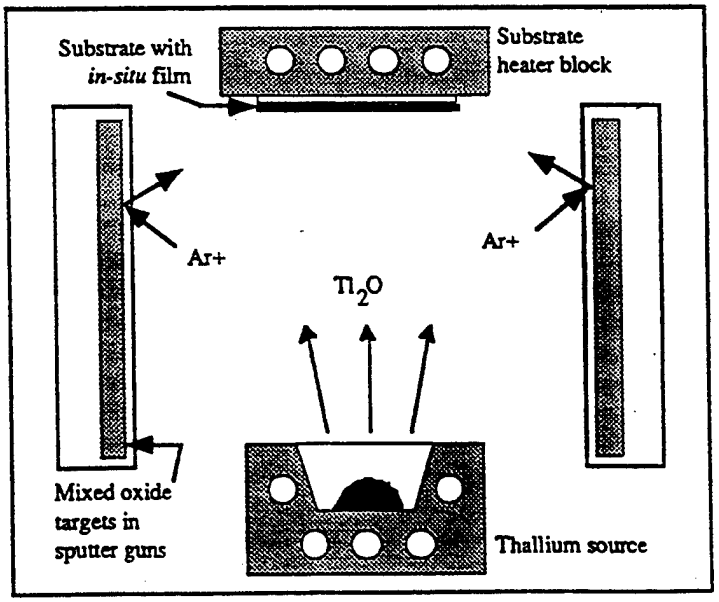


Figure 2: Schematic of the *in situ* thallium deposition chamber.

As demonstrated in Section 2, high partial pressures of $Tl_2O$ are required for the vapor phase deposition of crystalline thallium cuprates, or other thallium-containing oxides. The thallium source that has been developed to provide this high $P_{Tl2O}$ is a thermal source: a resistively-heated nickel crucible with a central cavity for loading $Tl_2O_3$ powder.[18] The other cations are deposited by off-axis RF magnetron sputtering from a mixed oxide target. A schematic of the deposition chamber is shown in Figure 2. The chamber has two sputter guns with 3" diameter targets which are situated in opposition, about 13 cm apart. The substrates are attached with silver paint to a resistively-heated nickel block located between the guns, 3.5 cm above the center line of the targets.

Defining the output of the thallium source is problematic. The source is charged with several grams of thallic (III) oxide, $Tl_2O_3$. As noted above, under an oxygen partial pressure of 100 mtorr, $Tl_2O_3$ is stable up to about 450 °C. At higher temperature it converts to the mixed valence compound, $Tl_4O_3$. Both the $Tl_4O_3$ and $Tl_2O_3$ phases decompose to produce $Tl_2O(g)$ and O2(g) depending on $P_{O2}$ and temperature. A water-cooled quartz crystal monitor is situated above the thallium source and to the side of the substrates. The oxidation state of the thallium that condenses on the cool quartz crystal is unknown. In order to convert the measured frequency shift of the quartz crystal monitor to a deposition rate, one needs to know the density of the material deposited. For this purpose, a density of 10.0 g/cm$^3$ has been assumed for the condensed phase, $TlO_x$. For comparison, the density of $Tl_2O_3$ is reported to range from 9.65 g/cm$^3$ for amorphous material to 10.19 g/cm$^3$ for single crystals and the density of $Tl_2O$ is 9.52 g/cm$^3$.[19] The deposition rate thus calculated is referred to as the "thallium oxide volatilization rate" in this and earlier publications. Feedback from the crystal monitor is used to adjust the thallium source temperature.

The sputtering gas was a mixture of Ar and either $O_2$ or $N_2O$. Nitrous oxide may be used to enhance the concentration of monatomic oxygen in the plasma since the $N_2$-O bond is weaker than the O-O bond. The total pressure was kept at between 50 and 300 mtorr by means of a variable speed turbo pump. The substrates were heated to between 490 and 610°C in the sputtering gas. The thallium source temperature was ramped up at the same time. The thallium source is uncovered, so the substrates are exposed to a high thallous oxide vapor pressure prior to the deposition of the other elements. The 3" diameter sputter guns are run at 100 W RF power. Post-deposition pressure and temperature treatments varied for the different materials as described below.

## 4. THIN FILMS

Several different materials have now been successfully deposited by the *in situ* technique. Here the deposition process variations for the different materials are described. The first class of materials is the single Cu-$O_2$, single Tl-O layer materials, or the Tl-1201 phases. TlPb-1201 is an example of a non-superconducting metal made by the *in situ* process. Most work to date has been done on the Tl-1212 materials, as discussed in Section 4.2. In the next section, recent work by Reschauer *et al.* on the TlBa-1223 material is overviewed. In Section 4.4, the prospects for deposition of the double Tl-O layer cuprates are discussed. Finally, in Section 4.5, new work is reported on $Tl_2Ta_2O_6$, an insulating material with the pyrochlore structure. Thallium tantalate is well lattice-matched to the thallium cuprates and may be interesting as a buffer layer or insulator in multilayer devices.

### 4.1. Tl-1201

Stoichiometric $TlBa_2Cu_2O_5$ and $Tl_{0.5}Pb_{0.5}Sr_2CuO_5$ are not superconducting. The formal oxidation state of the copper is 3.0+ and 2.5+ for the TlBa-1201 and TlPb-1201 phases, respectively, placing them well into the over-doped regime. Oxygen depletion can be used to make these materials superconducting at up to 10 K. Transition temperatures of up to 44 K can be achieved with substitution of a trivalent rare earth on the Ba or Sr site.

TlPb-1201 is stable over a fairly broad range of temperature, $P_{O2}$, and composition. It was often seen as an impurity phase in TlPb-1212 films grown under non-optimal conditions. Using targets of composition $Pb_{1.6}Sr_2CuO_x$ allowed the fabrication of phase-pure TlPb-1201 films.[13] Excess lead in the targets was necessary to compensate for the low sticking coefficient, or high volatility,[20] of lead. The best TlPb-1201 films were deposited at a substrate temperature ($T_s$) of 595 °C, a bit higher than is optimal for the TlPb-1212 phase. The optimal thallium oxide volatilization rate is about 24 Å/min., 20% lower than that for TlPb-1212. After deposition, the chamber was backfilled with $N_2O$ to 500 torr, and the films cooled to room temperature directly.

The structural properties of these TlPb-1201 films are excellent. Figure 3a is an x-ray diffraction θ-2θ scan for a $(Tl,Pb)Sr_2CuO_5$ film on (100) $LaAlO_3$. The primary peaks are the 00$\ell$ reflections of the TlPb-1201 phase, indicating that the film is c-axis oriented. A Φ-scan through the 103 reflection of the same film is shown in Figure 3b. The average width (FWHM) of the 103 peaks is 0.9° and they are rotated 45° from the 202 peaks of the $LaAlO_3$ substrate. This demonstrates a strong in-plane alignment of the <100> axes of the TlPb-1201 film with the pseudo-cubic <100> axes of the $LaAlO_3$ substrate. The resistivity of these epitaxial TlPb-1201 films is in the milliohm-cm range and is weakly temperature-dependent.

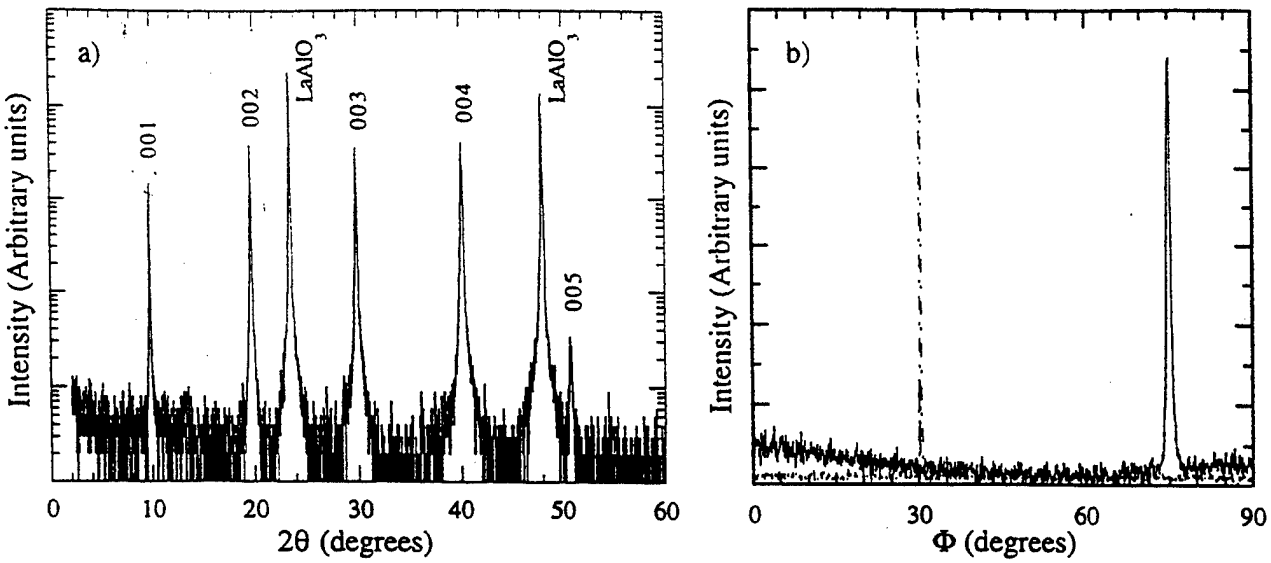


Figure 3: X-ray diffraction data for a TlPb-1201 film on (100) $LaAlO_3$: a) θ-2θ scan and b) phi scan through the 103 reflection of TlPb-1212 (solid line) and the 202 reflection of $LaAlO_3$ (dashed line).

There has not, to this author's knowledge, been an attempt to make TlBa-1201 thin films. The TlBa-1201 phase was not observed as an impurity peak in the growth of TlBa-1212 films on $LaAlO_3$ or $NdGaO_3$ over a range of temperatures, $P_{O2}$, or thallium oxide volatilization rate. "Very small amounts" were seen in films on MgO, where the TlBa-1212 phase did not form.[21] Clearly the formation of TlBa-1201 is not especially favorable over a large range of composition as is that of TlPb-1201.

4.2 Tl-1212

High quality epitaxial thin films of both $TlBa_2CaCu_2O_7$ (TlBa-1212) and $(Tl,Pb)Sr_2CaCu_2O_7$ (TlPb-1212) have been made by the *in situ* process. TlBa-1212 has a transition temperature of 90 K and up to 100 K when doped with a rare earth on the calcium site.[22] Likewise, the transition temperature of $(Tl,Pb)Sr_2Ca_{1-x}Y_xCu_2O_7$ varies as a function of the yttrium doping level, from 85 K at x = 0 up to 108 K for x = 0.2.[23,24]

An interesting feature, and key difference between TlBa-1212 and TlPb-1212 is their relative sensitivities to oxygen anneal. Siegal *et al.* have shown that the transition temperature of *ex situ* TlBa-1212 thin films can be changed from about 70 K up to 87 K by annealing in nitrogen at 250 °C for one hour.[25] Such a dramatic change in $T_c$ at relatively low temperature indicates a high oxygen mobility in this material and raises questions about the long term stability of TlBa-1212. Conversely, the transition temperature of TlPb-1212 does not change even when the material is exposed to oxygen partial pressures from $10^{-4}$ to 1 atm. at temperatures up to 700 °C.[26,27] Indeed, no degradation in performance of *ex situ* TlPb-1212 films or microwave devices with time or repeated thermal cycling has been found in our laboratory. The absence of oxygen stoichiometry effects in *in situ* TlPb-1212 films has also been verified. No changes in the superconducting properties were seen after long anneals at 500 °C under pure Ar or under pure $N_2O$. This property of TlPb-1212 makes it an excellent candidate for use in Josephson Junctions, where the superconducting properties of the surface are critical.

The TlBa-1212 films were sputtered from $Ba_2CaCu_2O_x$ targets. The optimal growth conditions include a substrate temperature of 550 °C and a pressure of 200 mtorr. The sputter gas is a mixture of Ar and either $N_2O$ or $O_2$ in a 1:1 ratio, with the rates set by mass flow controllers. The thallium oxide volatilization rate was between 36 and 60 Å/min. After deposition, the thallium source was turned off and the chamber was filled to 500 torr with $O_2$. The samples were then *in situ* annealed at up to 725 °C for as long as 12 hours in pure $O_2$ without $Tl_2O$ vapor.[21]

The growth of TlPb-1212 films is complicated by the high vapor pressures of lead and the lead oxides, which are not as high as that of thallous oxide, but still appreciable. TlPb-1212 films were deposited at a substrate temperature of 580 °C. A target composition of $Pb_2Sr_2CaCu_2O_x$ produced films with compositions of approximately $Pb_{0.5}Sr_2CaCu_2O_x$ (noting that the relative lead loss is a strong function of $T_s$). The pressure and sputtering gases were the same as for TlBa-1212 except that the ratio between Ar and $N_2O$ was 1:2. The optimal thallium oxide volatilization rate was 30 Å/min. and the total deposition rate was about 7.8 Å/min. The backfill gas was either $N_2O$ or $O_2$.[12]

Samples cooled to room temperature immediately after deposition have the TlPb-1212 structure, indicating that this phase is formed during film growth. Figure 4a shows an x-ray diffraction θ-2θ scan for an unannealed $(Tl,Pb)Sr_2Ca_{0.8}Y_{0.2}Cu_2O_7$ film on (100) $LaAlO_3$. The primary peaks are the $00\ell$ reflections of the TlPb-1212 phase, indicating a c-axis oriented film. The as deposited films also contain small amounts of other oxides, such as $(Sr,Ca)PbO_3$ and $Pb_2O_3$, and the samples are not superconducting down to 30K.

After an *in situ* anneal at 750 to 800 °C for 60 to 120 min., again without further introduction of $Tl_2O$ vapor, the TlPb-1212 x-ray diffraction $00\ell$ peaks sharpen considerably as can be seen in Figure 4b. The ω-scan width (FWHM) of the 005 peak is 0.8°. Diffraction peaks due to the other phases disappear, and the films are superconducting at temperatures up to 94 K.

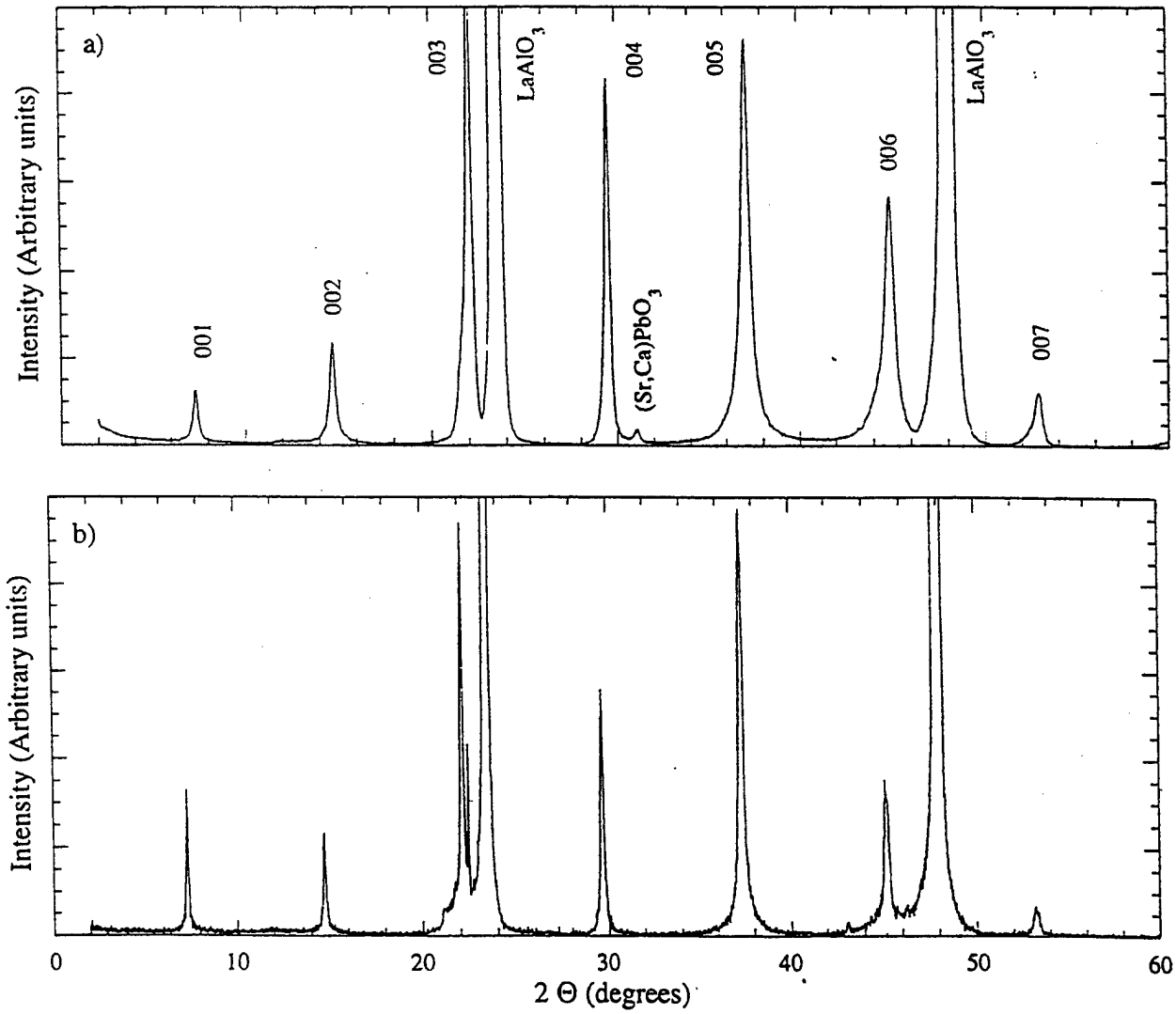


Figure 4: X-ray diffraction θ-2θ scans for TlPb-1212 films on (100) $LaAlO_3$ grown under identical conditions: a) as grown and b) after *in situ* anneal at 800 °C in $O_2$ for 60 min.

There is no apparent shift of the TlPb-1212 lines for unannealed or annealed samples, suggesting that the problem prior to anneal is one of cation disorder, not oxygen content.

One of the benefits of *in situ* deposition is that the films are generally smoother and have better connected, smaller grains. This has been verified for thin TlBa-1212 films where Atomic Force Microscopy (AFM) studies revealed a standard deviation surface roughness of about 20 Å.[21]

The transition temperatures of both TlBa-1212 and TlPb-1212 films increased with yttrium doping, as expected. The transition temperatures of TlBa-1212 films was elevated from around 70 K up to 97 K for a film with 20% yttrium doping. Thin films of $(Tl,Pb)Sr_2Ca_{1-x}Y_xCu_2O_7$ had transition temperatures of 82 and 94 K for x = 0 and x = 0.20, respectively.

Yttrium doping has another effect on both TlBa-1212 and TlPb-1212 films. Yttrium-doped films can be exposed to higher temperatures in the post-deposition anneal without suffering as much thallium loss as undoped films. Our anneals are done in a high oxygen partial pressure (0.66 atm.) in order to keep the thallous oxide vapor pressure low, even at elevated temperatures. Nevertheless, there is some thallium loss from the films. Undoped films must be annealed at lower temperatures and, as a result, their structural characteristics are not as good.

As mentioned in Section 2, knowledge of the partial pressure of $Tl_2O$ over the thallium cuprates as a function of temperature and $P_{O2}$ would be of great use in evaluating different fabrication processes. Obviously the thallium cuprate 1212 phases are stable at the growth conditions given above. Therefore, one can estimate the partial pressure of $Tl_2O$ over TlBa-1212 and TlPb-1212 for those conditions. The caveat is that the environment inside the deposition chamber is not homogeneous nor in equilibrium. There are surfaces at different temperatures, ranging from 580 ° C for the substrate to the water-cooled chamber walls. Argon and oxygen gases flow through the system. Thallous oxide is constantly generated and pumped away and also condenses on the chamber walls. In addition, there is the plasma of the sputter guns. The dynamic complexity of the process control parameter space is therefore further complicated by the inclusion of system geometry and physical size which requires a gallimaufry of detailed information to elucidate and define the idiosyncratic operating conditions. However, once defined, the process is reproducibly functional. The following are order-of-magnitude estimates and should be treated as such.

There are two ways to determine the partial pressure of thallous oxide inside the chamber during growth. The first, and most straightforward, is to recognize that the $Tl_2O$ is provided by a mass of condensed $TlO_x$ which is held at a certain temperature. Our thallium source is held at approximately 450°C, and is therefore just at the boundary between $Tl_2O_3$ and $Tl_4O_3$. Using the thermodynamic data of Ref. 9, one finds that the partial pressure of $Tl_2O$ over condensed $Tl_2O_3$ at 450 °C and in 100 mtorr $O_2$ is about $8 \times 10^{-2}$ mtorr ($1 \times 10^{-7}$ atm).

A second method is to consider the deposition rate of $TlO_x$ onto the water-cooled quartz crystal monitor. The deposition rate during growth is 30 to 60 Å/min. It is assumed that the velocity of the $Tl_2O$ vapor is "thermallized," i.e. it has the same velocity as the other gases in the chamber. The average velocity of the argon (or $O_2$) molecules can be determined from kinetic gas theory:[28]

$$\left\langle v_{Ar}^2 \right\rangle^{1/2} = \left( \frac{3RT}{M_{Ar}} \right)^{1/2} \tag{3}$$

where $v_{Ar}$ is the velocity of the Ar atoms, M is molecular weight, and T is temperature, which is taken to be 450 °C. Then the partial pressure of the thallous oxide is:

$$P_{Tl2O} = \frac{1}{3}\frac{mN}{V} v_{Tl2O}^2 = \frac{1}{3}\frac{M_{Tl2O}}{N_0}\left(\frac{R_d}{A}\right) v_{Tl2O} \tag{4}$$

where m is the mass of $Tl_2O$ molecules, N is the number of molecules per a volume V, $N_O$ is Avogadro's number, and $(R_d/A)$ is the deposition rate per unit area. The deposition rate per unit area is calculated from the $TlO_x$ deposition rate (in Å/min.) and the unit cell volume of the condensed phase, which is assumed for the moment to be $Tl_2O_3$. This calculation gives a partial pressure of $8 \times 10^{-3}$ mtorr ($1 \times 10^{-8}$ atm). These two independent methods give similar values, giving confidence to the

estimate. The calculated partial pressure of $Tl_2O$ over condensed thallium oxide at 580 °C and 100 mtorr $O_2$ is 3 x $10^{-4}$ atm. Thus, $P_{Tl2O}$ over TlBa-1212 or TlPb-1212 is $10^3$ to $10^4$ times lower than that over $TlO_x$ for our temperature and $P_{O2}$ conditions. We note that the fact that some of the thallium is ionized, due to the presence of the sputtering plasma, may lower the total partial pressure of $Tl_2O$ required to stablize the cuprates.

4.3 Tl-1223

Recently Reschauer *et al.* reported the first *in situ* growth of $TlBa_2Ca_2Cu_3O_9$ (TlBa-1223) thin films.[14] These films were made by pulsed laser deposition in the presence of thermally-generated thallous oxide. One advantage of laser deposition relevant to the growth of thallium-containing materials is that the process can be done at higher pressure. For the thallium cuprates, this allows the use of higher substrate temperatures for a given $P_{Tl2O}$ or lower $P_{Tl2O}$ for a set $T_s$. In this case, the oxygen pressure during growth was 3 mbarr (2.5 torr), a factor of ten higher than can be used during sputter deposition. The TlBa-1223 films were reported to be highly c-axis oriented, with small amounts of TlBa-1212 as an impurity phase. The films had smooth surfaces and transition temperatures near 100 K. This is an exciting development as the maximum $T_c$ for bulk TlBa-1223 is 120 K.[29]

4.4 Double Tl-O layer compounds

The $Tl_2Ba_2Ca_{n-1}Cu_nO_{2n+4}$ family of materials is interesting for several reasons. The n = 3 member has a $T_c$ of 125 K, the highest among the thallium cuprates.[30] All of these materials have fairly weak flux pinning, a property associated with the double Tl-O sheets and the resultant large gap between Cu-$O_2$ sheets. Weak flux pinning is desirable in certain electronic devices such as the flux-flow transistor. Additionally, a good technology base already exists for TlBa-2212. *Ex situ* TlBa-2212 thin films are widely studied and the superconducting properties of this material are known to be excellent.

There has not been any success to date in the *in situ* fabrication of phase-pure double Tl-O layer thin films. The work of Aselage *et al.*[16] showed that for high $O_2$ partial pressures, the partial pressure of $Tl_2O$ required to stabilize the double Tl-O layer cuprates is higher than is that required for the single Tl-O layer phases. Simply increasing the thallium deposition rate over that used to grow TlBa-1212 (or TlPb-1212) leads to the formation of Tl-rich phases and $Tl_2O_3$, but not to growth of TlBa-2212 (or TlPb-2212). However, TlBa-2201 was seen as an impurity phase in TlBa-1212 films grown over a variety of conditions.[21] Surprisingly, it was seen at lower temperatures and thallium oxide volatilization rates than was TlBa-1212. The transition temperature of TlBa-2201 varies with fabrication process, from zero to 90 K. High quality thin films of this material would be interesting both for basic materials research and technical applications.

4.5 $Tl_2Ta_2O_6$

Thallium tantalate is an insulator of the pyrochlore structure. It has a cubic lattice constant of 10.61 Å, which can provide a good lattice match to the thallium cuprates (10.61Å / 2 $\sqrt{2}$ = 3.75 Å). Unfortunately, there is little other information about this material in the literature.[31]

The DuPont group has recently grown $Tl_2Ta_2O_6$ thin films on a variety of substrates including $LaAlO_3$, $NdGaO_3$, and yttria-stabilized zirconia (YSZ). For these depositions, tantalum metal targets and a thallium oxide volatilization rate of 12 Å/min. were used. The sputter gas was a mixture of 90% Ar and 10% $O_2$ at a pressure of 200 mtorr. The substrate temperature was 595 °C and the samples were cooled to room temperature immediately after deposition. The chamber was backfilled with 500 torr oxygen during the cool-down.

Figure 5 shows x-ray diffraction data for a $Tl_2Ta_2O_6$ film on (100) YSZ. In the θ-2θ scan, the two main peaks from the film are *h*00 reflections indicating good (100) orientation. Figure 5b is a Φ scan through the 440 reflections of the $Tl_2Ta_2O_6$ film, where the zero point of Φ corresponds to the in-plane <010> axes of the YSZ. Peaks are only seen at zero and 90° intervals indicating epitaxial, cube-on-cube growth.

Thallium tantalate may be useful in the fabrication of thallium-based multilayer devices. The fact that high quality thin films of $Tl_2Ta_2O_6$ can be made by the *in situ* process under conditions similar to those used for the thallium cuprates is very encouraging. Details on the growth and dielectric properties of $Tl_2Ta_2O_6$ thin films on different substrates will be published separately.

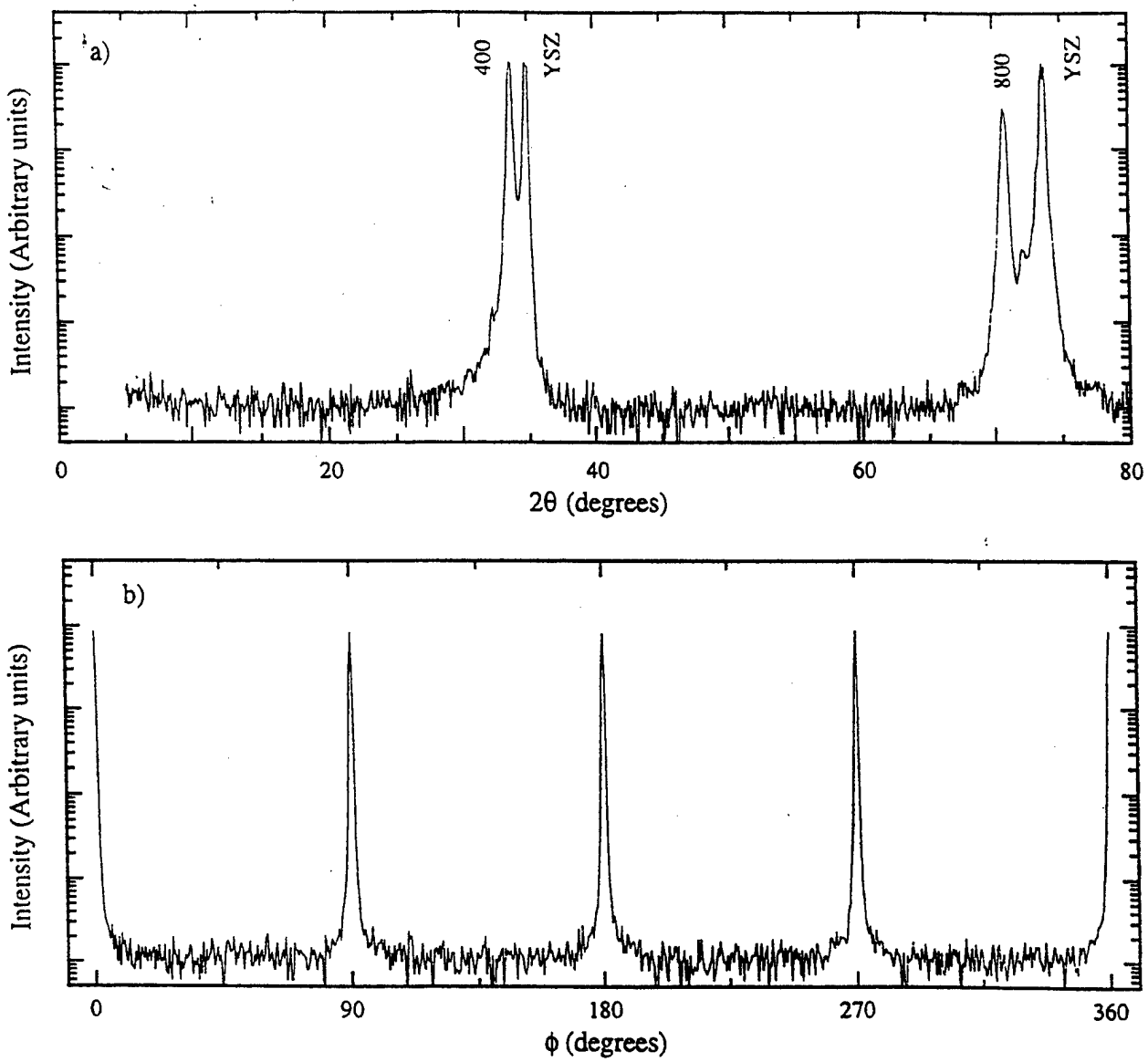


Figure 5: X-ray diffraction data for a $Tl_2Ta_2O_6$ film on (100) YSZ: a) θ-2θ scan and b) phi scan through the 440 reflections of $Tl_2Ta_2O_6$.

## 5. MULTILAYERS

*In situ* deposition has enabled the growth of thallium-containing multilayers. The ability to grow epitaxial thallium cuprate multilayers brings with it the potential for making thallium cuprate multilayer Josephson Junctions and other complex circuits. A great deal of work will need be done to realize that potential, but the groundwork has been laid and the experience gained from research on other HTS materials will guide the effort.

### 5.1 TlBa-1212/$CeO_2$

The first multilayer, *in situ* thallium cuprate structures were bilayers of TlBa-1212 and $CeO_2$.[11] $TlBa_2Ca_{0.75}Y_{0.25}Cu_2O_7$ films were grown under the standard conditions given in section 4.2. Cerium oxide films, 500 Å thick, were deposited in the same

chamber, but in a separate run. The substrate temperature during $CeO_2$ growth could be varied from 450 °C to 525 °C without degradation of the superconducting properties of the underlying TlBa-1212 layer. However, introduction of $Tl_2O$ vapor, during either the $CeO_2$ growth or attempts to deposit a TlBa-1212 film on top of the bilayer, seemed to cause reaction between the various layers. Thus trilayer structures of TlBa-1212 and CeO2 were not possible.

5.2 TlPb-1212/1201

Trilayer structures have been successfully made with the thallium lead cuprates. An SNS structure was grown in two successive runs using TlPb-1212 as the superconducting layers and TlPb-1201 as the normal metal. During the first run a bilayer of TlPb-1201 on TlPb-1212 was made. The TlPb-1212 layer was annealed before depositing the TlPb-1201 layer. The anneal turned out to be important, presumably because it improves the template for the TlPb-1201 growth. At the end of the deposition, the chamber was filled to a pressure of 500 torr with $N_2O$ and the samples cooled as usual.

The second TlPb-1212 deposition was done with two edges of the bilayer film covered to avoid deposition and allow electrical characterization of the individual TlPb-1212 layers. All three layers grew in the c-axis orientation and with in-plane alignment of their major crystallographic axes. The upper and lower layers were both superconducting with transition temperatures of 94 and 93 K, respectively.[13]

## 6. SUMMARY

The thallium cuprate superconductors have many aspects which make them attractive for commercial use. They have high transition temperatures, up to 125 K, low surface resistances,[32] and excellent microwave power handling capability.[33] Thallium cuprates are also environmentally more robust than other HTS materials. The three different families of materials, $TlBa_2Ca_{n-1}Cu_nO_{2n+3}$, $Tl_2Ba_2Ca_{n-1}Cu_nO_{2n+4}$, and $(Tl,Pb)Sr_2Ca_{n-1}Cu_nO_{2n+3}$, have similar structure and chemistry.[34] A thallium-based materials technology would enable the exploitation of the different properties of the various phases.

Consistent progress is being made in this direction. Thallium-based superconductors, normal metals, and insulators can now all be deposited by *in situ* techniques. Multilayer structures have been successfully fabricated. Work in this area will continue and hopefully increase so as to realize thallium cuprate active devices and bring closer the development of thallium cuprate-based multilayer circuitry.

## 7. ACKNOWLEDGMENTS

The author would like to thank Dean Face and Paul Martin for helpful discussions and their critical review of this manuscript and Professors Darrell Schlom and Susan Trolier-McKinstry, both of The Pennsylvania State University, for their analysis of the thallium tantalate films.

## 8. REFERENCES

[1] Z. Z. Sheng and A. M. Hermann, Nature 332, 138 (1988).
[2] Jack Browne, Microwaves and RF, July, 1993.
[3] F. C. Wellstood, J. J. Kingston, and John Clarke, J. Appl. Phys. 75, 683 (1994).
[4] J. S. Martens, V. M. Hietala, T. E. Zipperian, G. A. Vawter, D. S. Ginley, C. P. Tigges, T. A. Plut, and G. K. G. Hohenwarter, Appl. Phys. Lett. 60, 1013 (1992).
[5] J.P. Hong, H.R. Fetterman, R.J. Forse, and A. H. Cardona, Appl. Phys. Lett. 62, 2865 (1993).
[6] A. H. Cardona, H. Suzuki, K. H. Young, and L. C. Bourne., Appl. Phys. Lett. 62, 411 (1993).
[7] R. Kleiner and P. Müller, Phys. Rev. B 49, 1327 (1994); F. Schmidt, A. Pfuch, H. Scheidewind, E. Heinz, L. Dörrer, A. Matthes, P. Seidel, U. Hübner, M. Veith, and E. Steinbeiß, Supercon. Sci. Tech. 8, 740 (1995).
[8] R. B. Laibowitz, R. H. Koch, A. Gupta, G. Koren, W. J. Gallagher, V. Foglietti, B. Oh, and J. M. Viggiano, Appl. Phys. Lett. 56, p. 686, 1990.
[9] W. L. Holstein, J. Phys. Chem. 97, 4224 (1993).
[10] D. W. Face and J. P. Nestlerode, Appl. Phys. Lett. 61, 1838 (1992).

[11] D. W. Face, D. J. Kountz, and J. P. Nestlerode, "In-situ Growth and Properties of Epitaxial $TlBa_2(Ca_{1-x}Y_x)Cu_2O_7$ Films and Multilayers"in *Advances in Superconductivity VI*, T. Fujita and Y. Shinohara, Eds., p.863., Springer-Verlag, Tokyo, 1994.
[12] K. E. Myers, D. W. Face, D. J. Kountz, and J. P. Nestlerode, Appl. Phys. Lett. 65, 490 (1994).
[13] K. E. Myers, D. W. Face, D. J. Kountz, J. P. Nestlerode, and C. F. Carter, IEEE Trans. on Appl. Supercond. 5, 1684 (1995).
[14] N. Reschauer, A. Piehler, U. Spreitzer, K. F. Renk, R. Berger, and G. Saemann-Ischenko, presented at the European Conference on Applied Superconductivity, Edinburgh, Scotland, July 3-6, 1995.
[15] T. L. Aselage, J. A. Voigt and K. D. Keefer, J. Am. Ceram. Soc. 73, 3345 (1990); T. L. Aselage, J. A. Voigt, E. L. Venturini, W. F. Hammetter, S. B. VanDeusen, D. L. Lamppa, R. G. Tissot, M. O. Eatough, and K. D. Keefer, Ceram. Trans. 18, 9 (1991); T. L. Aselage, E. L. Venturini, S. B. VanDeusen, T. J. Headley, M. O. Eatough and J. A. Voigt, Physica C 203, 25 (1992).
[16] T. L. Aselage, E. L. Venturini, and S. B. Van Deusen, J. Appl. Phys. 75, 1023 (1994).
[17] W. L. Holstein, Appl. Supercond. 5, 345 (1994).
[18] D. W. Face, U.S. patent # 5,389,606.
[19] *Handbook of Chemistry and Physics*, Robert C. Weast, Ed., p. B-148, CRC Press, Boca Raton, Florida, 1984.
[20] R. H. Lamoreaux, D. L. Hildenbrand, and L. Brewer, J. Phys. Chem. Ref. Data 16, 419 (1987).
[21] D. W. Face and J. P. Nestlerode, IEEE Trans. on Appl. Supercond. 3, 1516 (1993).
[22] S. Nakajima, M. Kikuchi, Y. Syono, N. Kobyashi, and Y. Muto, Physica C 168, 57, 1990.
[23] M.A. Subramanian, C.C. Torardi, J. Gopalakrishnan, P.L. Gai, J.C. Calabrese, T.R. Askew, R.B. Flippen, and A.W. Sleight, Science 242, p. 242, 1988.
[24] J.M. Liang, R.S. Liu, Y.T. Huang, S.F. Wu, P.T. Wu, and L.J. Chen, Physica C 165, p. 347, 1990.
[25] M. Siegal, E. L. Venturini, P. P. Newcomer, B. Morosin, D. L. Overmyer, F. Dominguez, and R. Dunn, Appl Phys Lett. 67, 3966 (1995).
[26] J.L. Tallon, R.S. Liu, K.L. Wu, F.J. Blunt, and P.T. Wu, Physica C 161, p. 523, 1989.
[27] M.R. Presland, J.L. Tallon, R.G. Buckley, R.S. Liu, and N.E. Flower, Physica C 176, p.95, 1991.
[28] Ignacio Tinoco, Jr., Kenneth Sauer, and James C. Wang, *Physical Chemistry*, p. 221, Prentice-Hall, Englewood Cliffs, NJ, 1985.
[29] C. Martin, C. Michel, A. Maignan, M. Hervieu, and B. Raveau, C.R. Acad. Sci. Paris 307, Ser. II, 27 (1988).
[30] C. C. Torardi, M. A. Subreamanian, J. C. Calabrese, J. Gopalakrishnan, T. R. Askew, R. B. Flippen, U. Chowdhry, and A. W. Sleight, Science 240, 631 (1988).
[31] Marcel Ganne and Michel Tournoux, Mat. Res. Bull. 10, 1313 (1975).
[32] A. Lauder, C. Wilker, D. J. Kountz, W. L. Holstein, and D. W. Face, IEEE Trans. on Appl. Supercond. 3, 1683 (1993).
[33] Z. Y. Shen and Charles Wilker, Microwaves and RF, April, 1994.
[34] Charles G. Torardi, in *Chemistry of Superconductor Materials*, ed. Terrell A. Vanderah, Noyes Publications, Park Ridge, New Jersey, 1992, p. 485.